CONFIDENTIAL REPORT

XRD Results

Headwater Mineral Exploration and Development Ltd.
Heated/Glycolated/Potassium Saturated samples

Prepared for Headwater Mineral Exploration and Development Ltd.

By Ellen Friesen
Saskatchewan Research Council
Mining and Minerals Division

SRC Publication No. 10400-16C08
October, 2008

smart science solutions

CONFIDENTIAL REPORT

XRD Results

Headwater Mineral Exploration and Development Ltd.
Heated/Glycolated/Potassium Saturated samples

Prepared for Headwater Mineral Exploration and Development Ltd.

By Ellen Friesen
Saskatchewan Research Council
Mining and Minerals Division

SRC Publication No. 10400-16C08

October, 2008

Saskatchewan Research Council
125 – 15 Innovation Blvd.
Saskatoon, SK S7N 2X8
Tel: 306-933-5431
Fax: 306-933-7446

Appendix A

Analytical Conditions

XRD machine	Rigaku Miniflex +
X-ray tube	Cu
Scan Range	2° to 70°
Standard	Silica
Sample Mount	Heat: Random powder Glycol: Orientated slide Potassium Saturated: Oriented slide
Rotation	Rotation off to improve counting statistics.
Peak Identification Software	Jade v. 8
Mineralogical Database	International Centre Diffraction Data Pattern Diffraction File 4+2007 (PDF4+2007)
Quantitative Software	Rigaku Whole Pattern Fitting

Software Conditions
Jade v. 8 (ICDD PDF4+2007)

Condition	Application
Background	Cubic spline applied to background.
kα	Stripped

Results

Disclaimer: Due to uncertainty inherent in XRD analysis, the unambiguous identification of poorly crystalline and trace phases is not possible in all instances. In such cases, XRD analysis can, at best, provide an insight into phases that may be present in the sample. Mineral percentages derived by Rietveld analysis should be tempered with this information.

1. Heated Runs

By heating the sample, it is possible to eliminate some clays that may have overlapping peaks. . By heating to 550˚C, chlorite will increase in intensity and trioctahedral vermiculite and montmorillonite will collapse the d-spacing from 15 Å to 10 Å. For the wavelength of copper sourced radiation which was used on this project, this corresponds to 5.9 degrees to 8.8 degrees 2 Theta.

Heated runs of dried and hand-ground samples were heated to 550˚C and held at that temperature for a half an hour. The samples were then sealed in an airtight sample container until run to avoid humidity effects on the clays.

HW414- No change between heated and dry runs. This agrees with the rietveld analysis in which illite was the dominant clay mineral present.

HW415- No change between heated and dry runs. This agrees with the rietveld analysis in which illite was the dominant clay mineral present.

HW418- No change between heated and dry runs. This agrees with the rietveld analysis in which illite was the dominant clay mineral present.

HW422- Little change between heated and dry runs. This agrees with the rietveld analysis in which illite and kaolinite were the clay minerals present.

HW432- Little change between heated and dry runs. This agrees with the rietveld analysis in which illite and kaolinite were the clay minerals present.

HW433- Little change between heated and dry runs. This agrees with the rietveld analysis in which illite and kaolinite were the clay minerals present.

HW518- Dramatic change between heated and dry runs. The 15 Å peak is completely lost, and an increase in the intensity of the 10 Å peak occurs. This narrows the search to vermiculite and montmorillonite.

HW522- Dramatic change between heated and dry runs. The 15 Å peak is completely lost, and an increase in the intensity of the 10 Å peak occurs. This narrows the search to vermiculite and montmorillonite.

HW525- Dramatic change between heated and dry runs. The 15 Å peak is completely lost, and an increase in the intensity of the 10 Å peak occurs. This narrows the search to vermiculite and montmorillonite.

HW526- Dramatic change between heated and dry runs. The 15 Å peak is completely lost, and an increase in the intensity of the 10 Å peak occurs. This narrows the search to vermiculite and montmorillonite.

HW531- Dramatic change between heated and dry runs. The 15 Å peak is completely lost, and an increase in the intensity of the 10 Å peak occurs. This narrows the search to vermiculite and montmorillonite.

HW532- Dramatic change between heated and dry runs. The 15 Å peak is completely lost, and an increase in the intensity of the 10 Å peak occurs. This narrows the search to vermiculite and montmorillonite.

HW547- Dramatic change between heated and dry runs. The 15 Å peak is completely lost, and an increase in the intensity of the 10 Å peak occurs. This narrows the search to vermiculite and montmorillonite.

2. <u>Glycolated Runs</u>

Glycolation will differentiate between naturally occurring Mg-vermiculite and montmorillonite. Glycol will cause swelling of the montmorillonite reflection (001) to ~17.7 Å (Moore and Reynolds, 1989). The vermiculite will remain unaffected by the glycolation. The results would indicate that the d-spacing did expand, and therefore the major component is montmorillonite.

Glycolated runs were done by the saturation method, in which ethylene glycol was dripped onto a prepared smear mount slide. Excess glycol was dabbed off with a lab tissue or left in the fumehood until excess was no longer visible but the sample still appeared wet. Those samples with cation exchange capacity of 54 meq or greater were chosen for testing by ethylene glycol expansion.

HW518- Untreated peak at 15.7 Å, which expands to 17 Å with the ethylene glycol treatment.

HW522- Untreated peak at 15.2 Å, which expands to 16.7 Å with ethylene glycol treatment.

HW547- Untreated peak at 15.8 Å, which expands to 17 Å with ethylene glycol treatment.

3. Composition

The clay mineral of interest is likely montmorillonite with the potential of small amounts of illite interstratified throughout. A slight peak shift from the expected position could be explained by the presence of interstratified clay or it could be explained by the sources of error listed in the section below. Illite is found throughout the sample series and is commonly found in association with smectite as a diagenetic product (Howard, 1981). Rectorite, which is a regularly stratified smectite/illite clay, was found in a few samples.

The peak shifted well with the ethylene glycol saturation, suggesting that the composition is rich in smectite (Moore and Reynolds, 1989).

4. Sources of Error

Due to the nature of the samples, ideal sample preparation would have been extremely difficult to achieve. Samples were hand ground, and were not pulverized to the point of having uniform particle size. The crystalline non-clay minerals were left at a slightly larger size in order to preserve the structure of the clay minerals during grinding. Microabsorption effects will be present because of the particle size variation and the slight difference in mass attenuation coefficients between clay minerals and SiO_2 polymorphs (Madsen et al., 2001). Particle statistics, intensities, and error in precision will be affected, which in turn will affect the accuracy of semi-quantitative rietveld analysis. It was deemed that errors caused by particle size deviations would be less of an issue than destroyed clays.

Clays by their nature are difficult to quantify. It is rare in smectites to have well defined internal stacking that will have perfect translational order. Smectites are strongly susceptible to turbostratic stacking, in which the clay plates are randomly oriented, much like a disordered stack of cards (Moore and Reyolds, 1989). In smectites, non-rational basal plane reflections (001) caused by this mismatch results in peaks that are not well fitted to a calculated position (APDW, 2008). Smectites are particularly sensitive to slight variations due to their cation exchange capacity and different sized cations filling the interlayer space. Different hydration

states will affect the results, for example one or two water layers can be absorbed from the environment after drying and can coexist in one stack. As well, we see line broadening on the basal plane (001), which is a result of the long length, platy nature and orientation of the clay (APDW, 2008).

Rietveld algorithms have not been determined to take all the complexities of clay minerals into consideration, and therefore results should not be taken as highly accurate (Rienhard Kleeburg, Frieberg University, pers. communication, 2008)

5. References

APDW 2008 (Alberta Powder Diffraction Workshop) course notes: May 14-16th, 2008. University of Alberta.

Howard, J. 1981. *Lithium and potassium saturation of illite/smectite clays from interlaminated shales and sandstones.* Clays and Clay Minerals **29:**136-142.

Madsen, I., Scarlett, L., Cranswick, L., Lwin, T. 2001. *Outcomes of the Internation Union of Crystallography Commission on Powder Diffraction Round Robin on Quantitative Phase Anlaysis: samples 1a to 1h."* Journal of Applied Crystallography **34:**409-426.

Meunier, A., Lanson, B., Velde, B. 2004. *Composition variation of illite-vermiculite-smectite mixed-layer minerals in a bentonite bed from Charente (France).* Clay Minerals **39:**317-332.

Moore and Reynolds, 1989. *X-ray Diffraction and Identification and Analysis of Clay Minerals.* Oxford University Press. 332 p.

RAW AND HEATED X-RAY DIFFRACTOGRAMS

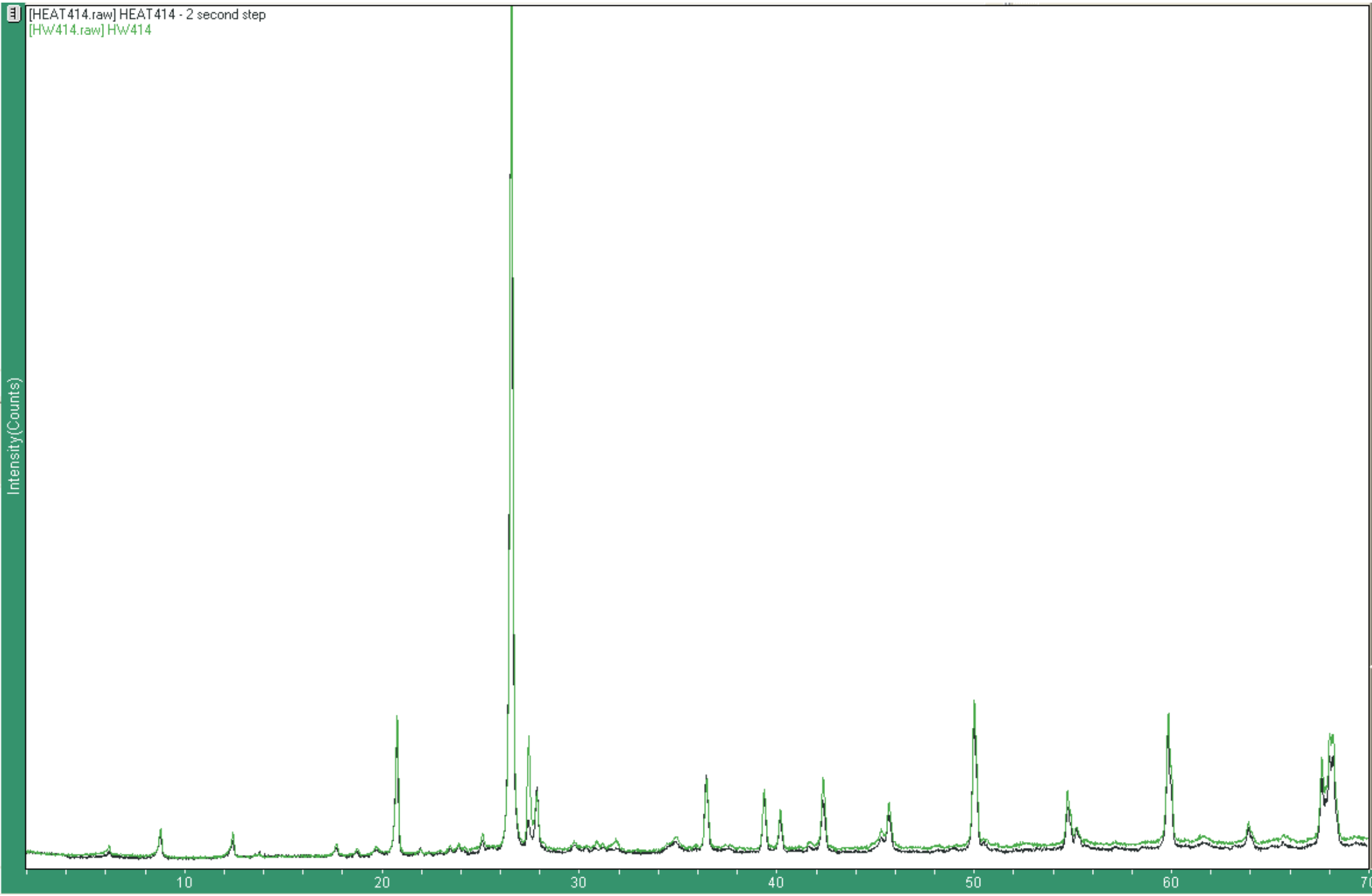
[HEAT414.raw] HEAT414 - 2 second step
[HW414.raw] HW414
Intensity(Counts)
10
20
30
40
50
60
70

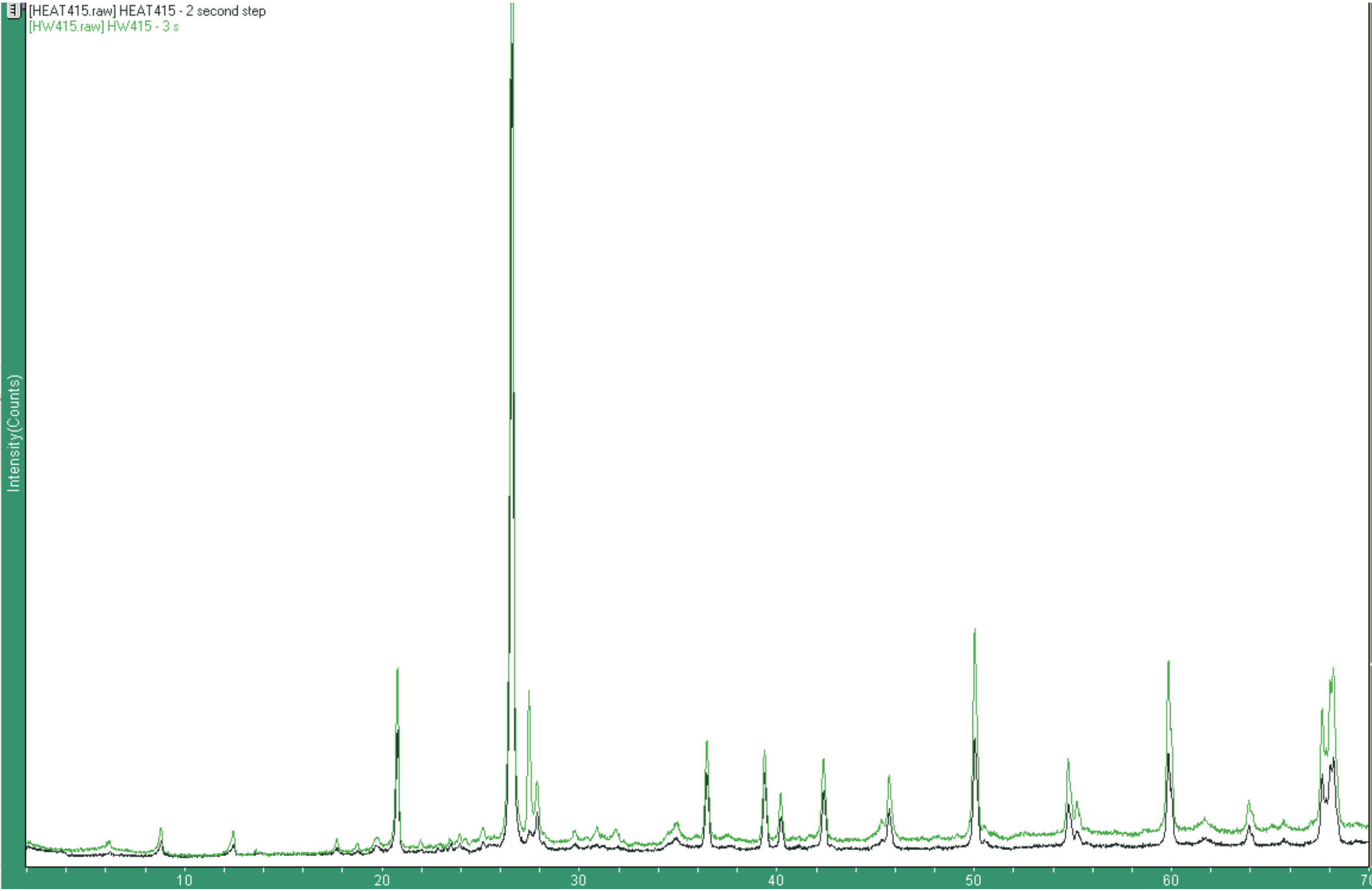
[HEAT415.raw] HEAT415 - 2 second step
[HW415.raw] HW415 - 3 s
Intensity(Counts)
10
20
30
40
50
60
70

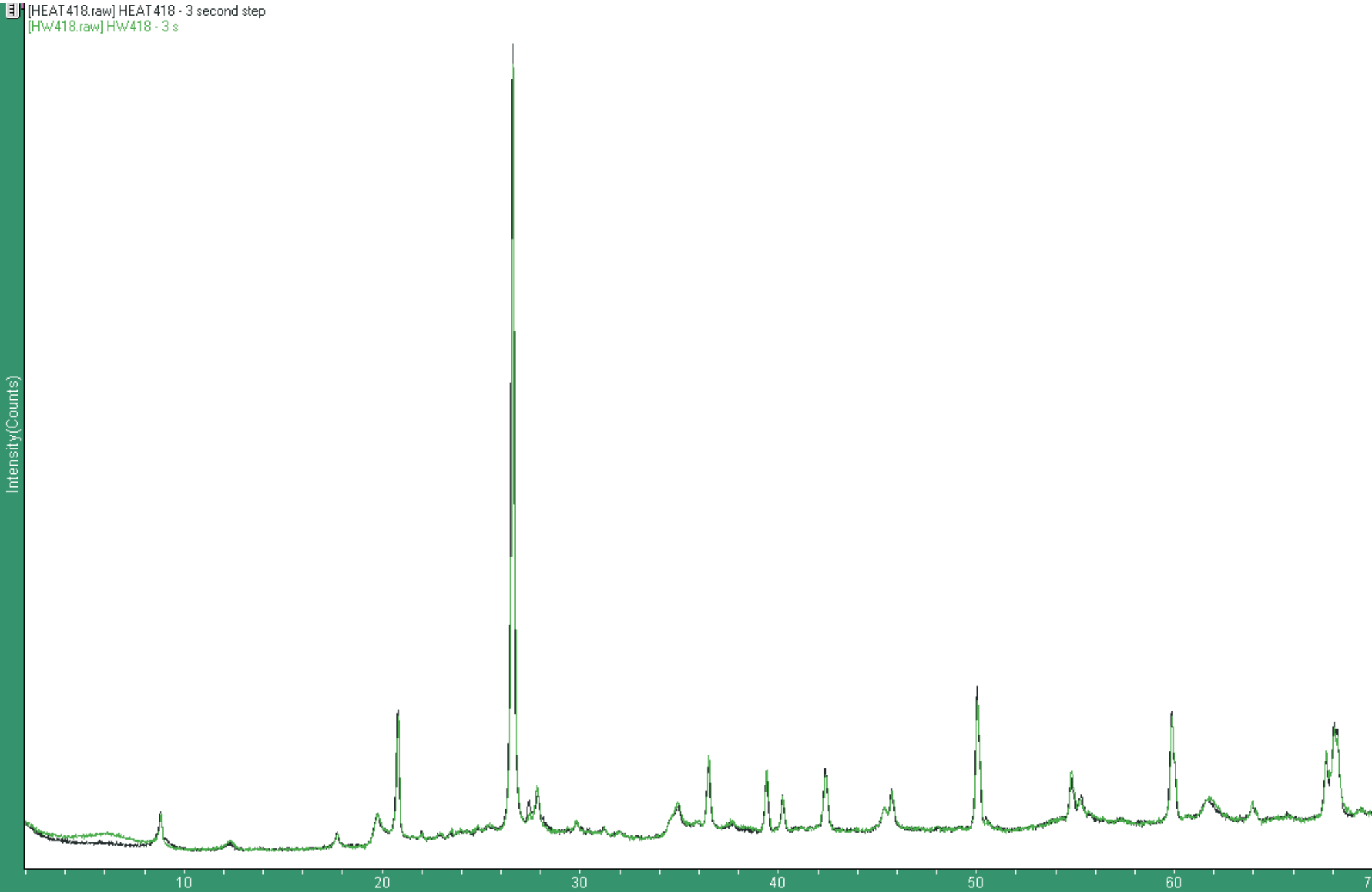
[HEAT418.raw] HEAT418 - 3 second step
[HW418.raw] HW418 - 3 s
Intensity(Counts)
10
20
30
40
50
60

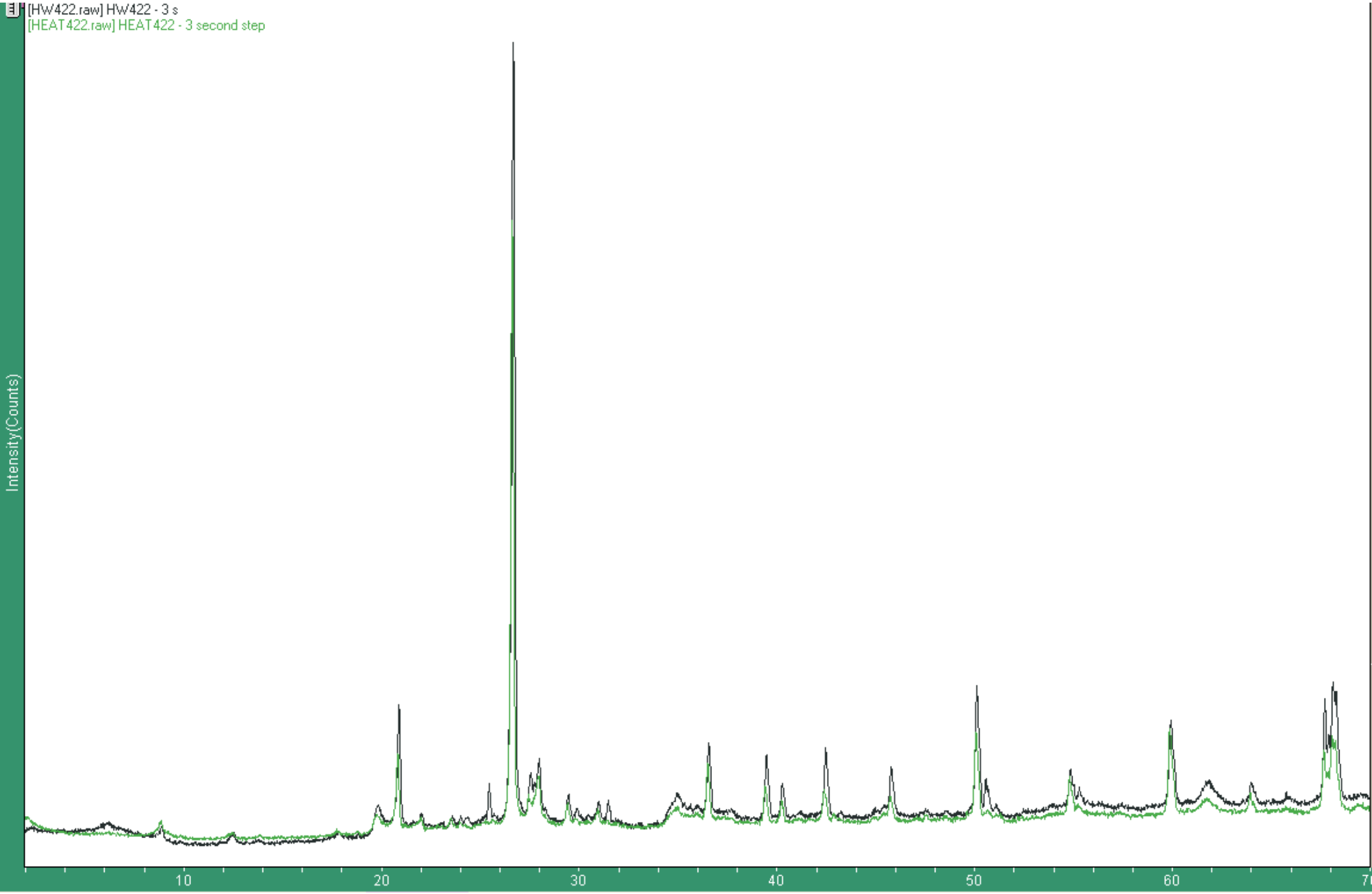
[HW422.raw] HW422 - 3 s
[HEAT422.raw] HEAT422 - 3 second step
Intensity(Counts)
10
20
30
40
50
60

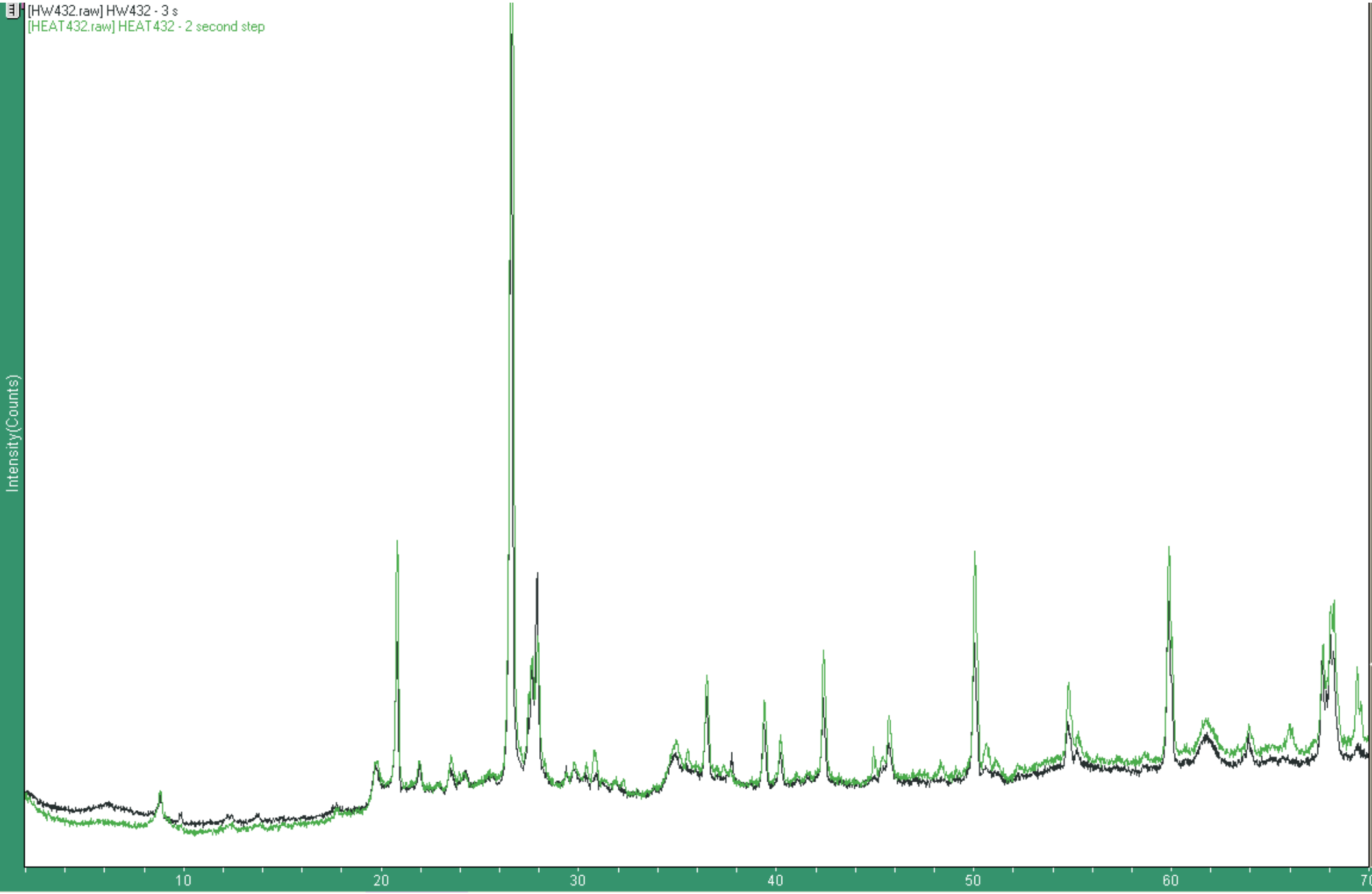
[HW432.raw] HW432 - 3 s
[HEAT432.raw] HEAT432 - 2 second step
Intensity(Counts)
10
20
30
40
50
60
70

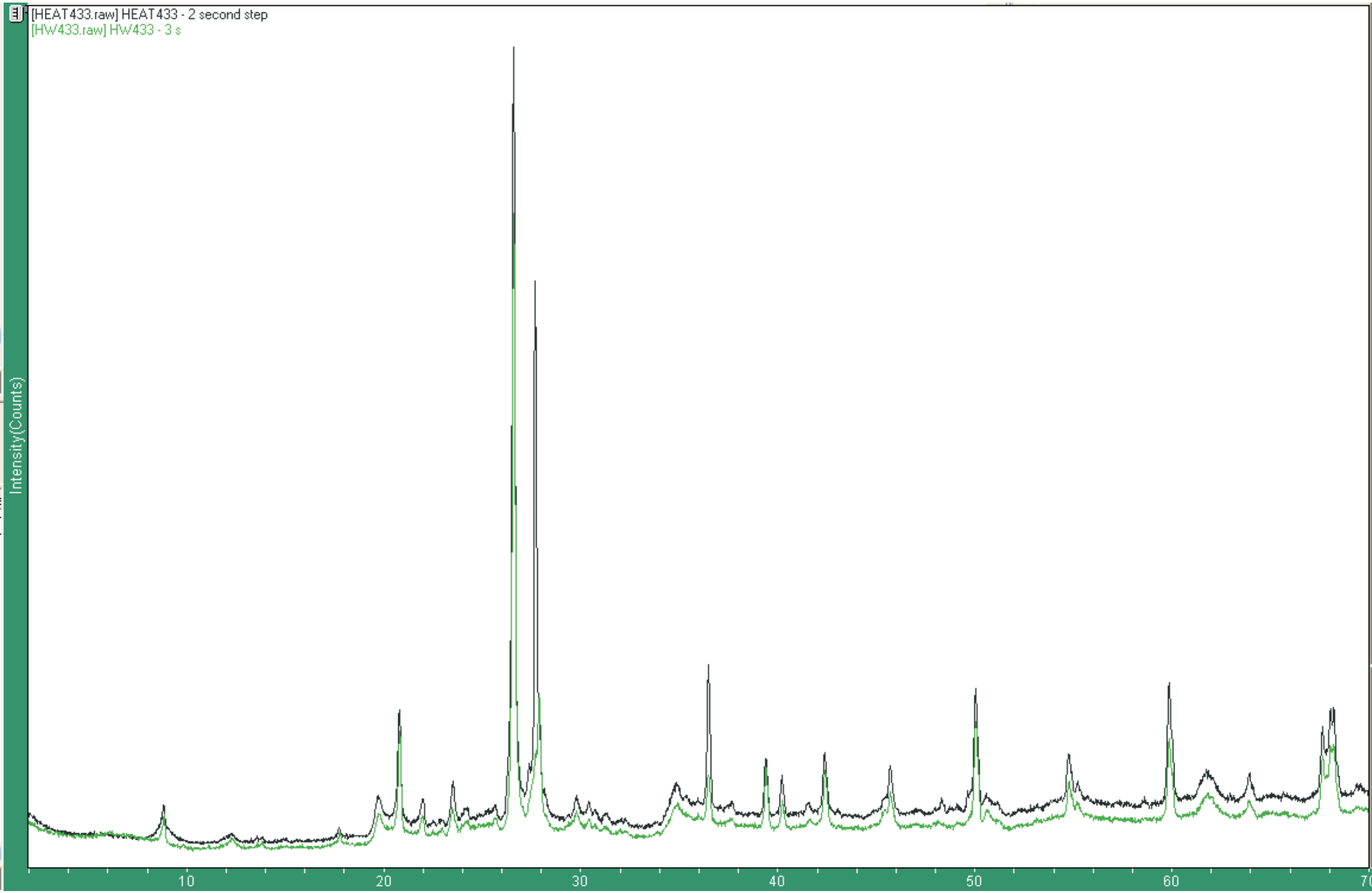
[HEAT433.raw] HEAT433 - 2 second step
[HW433.raw] HW433 - 3 s
Intensity(Counts)
10
20
30
40
50
60
70

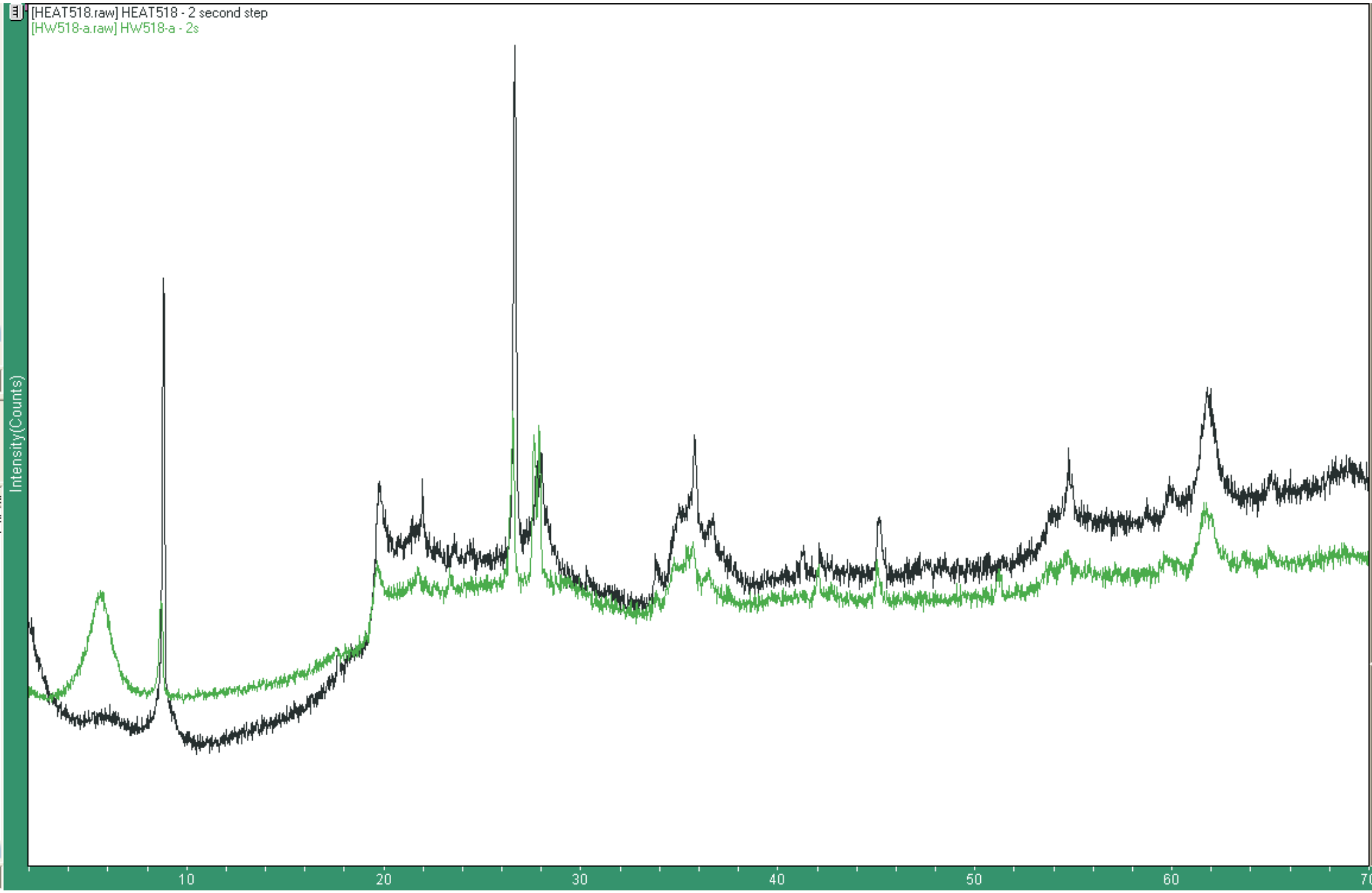
[HEAT518.raw] HEAT518 - 2 second step
[HW518-a.raw] HW518-a - 2s
Intensity(Counts)
10
20
30
40
50
60
70

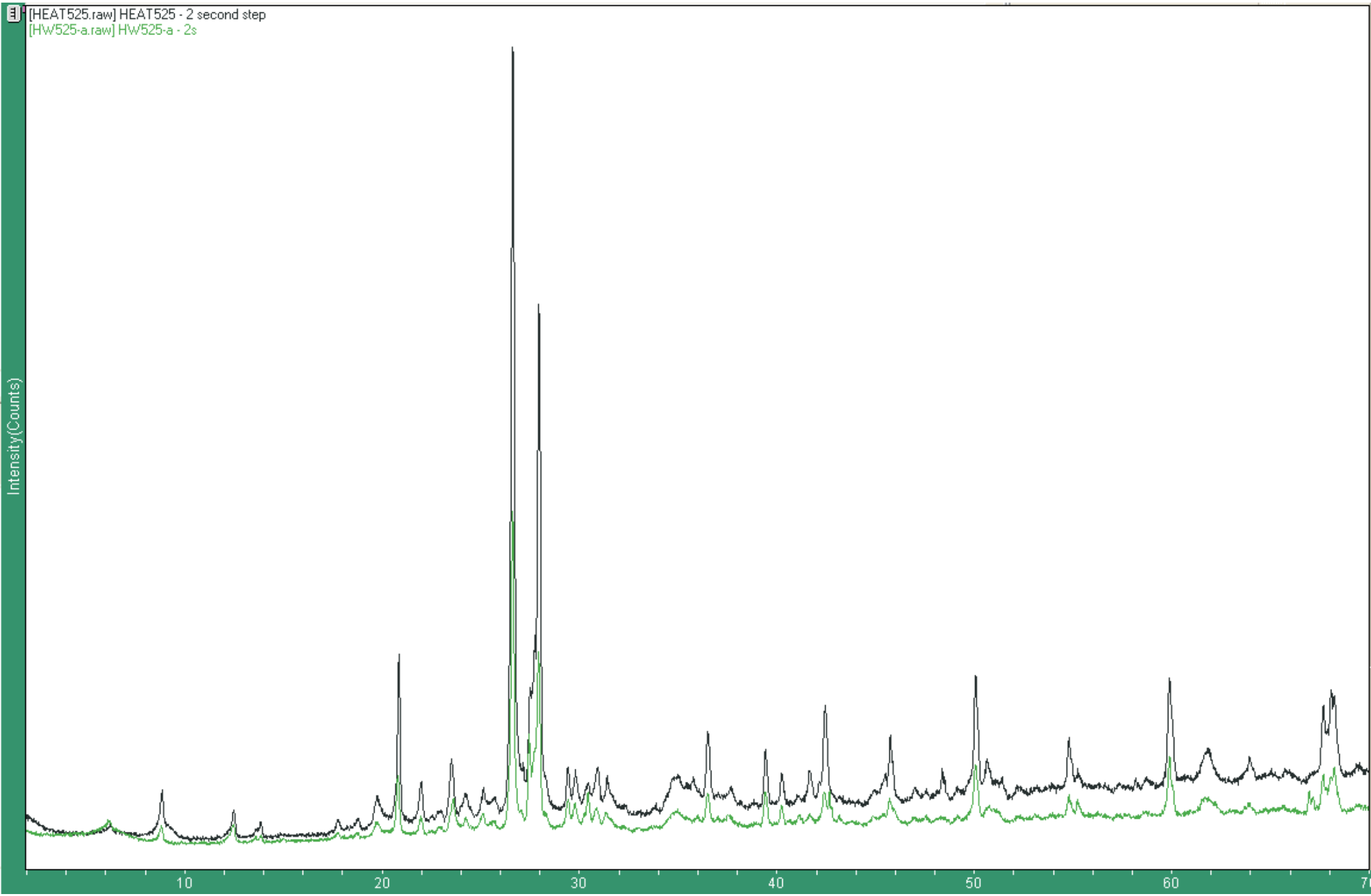
[HEAT525.raw] HEAT525 - 2 second step
[HW525-a.raw] HW525-a - 2s
Intensity(Counts)
10
20
30
40
50
60

HW526-heat comparison

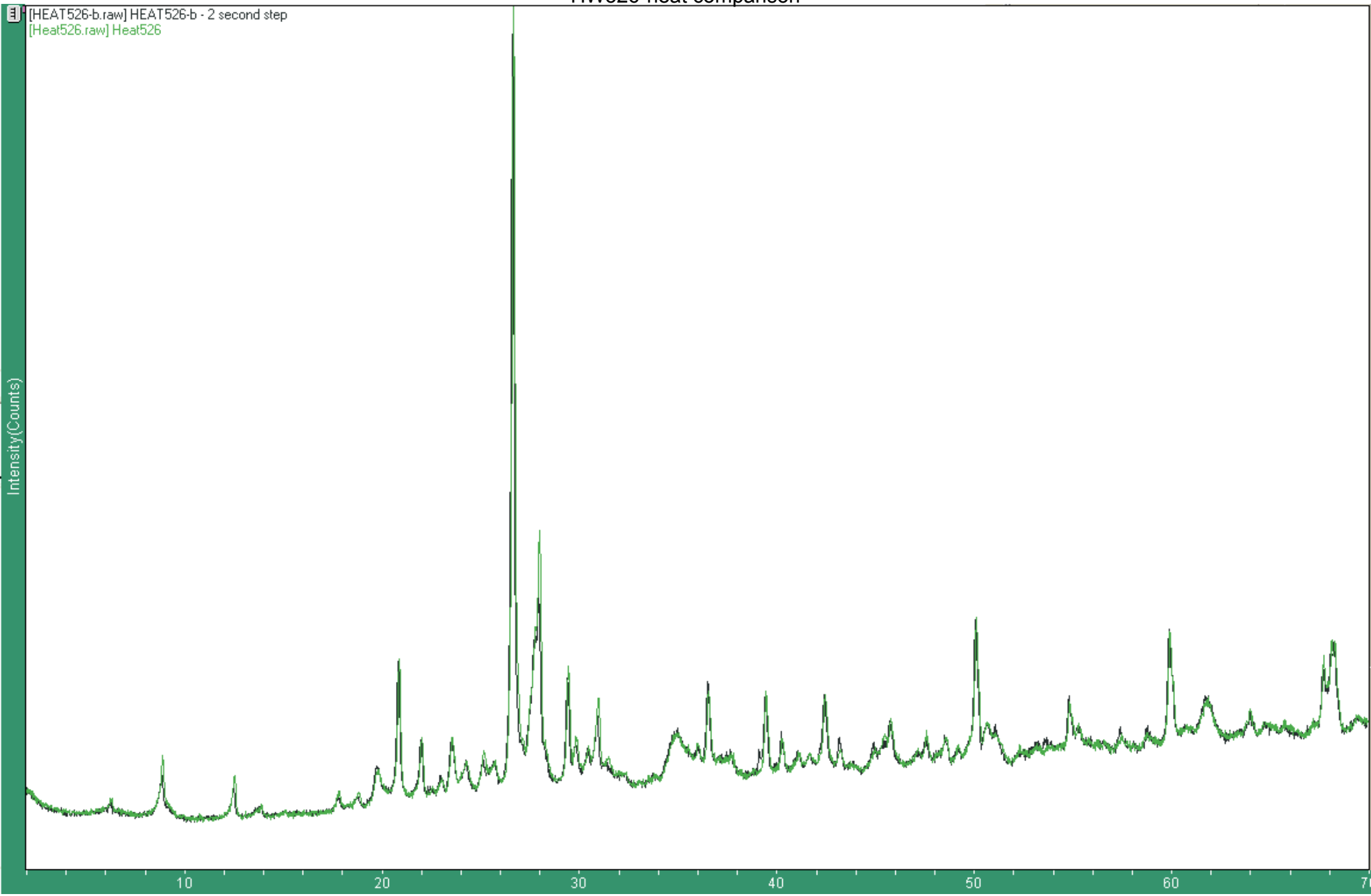

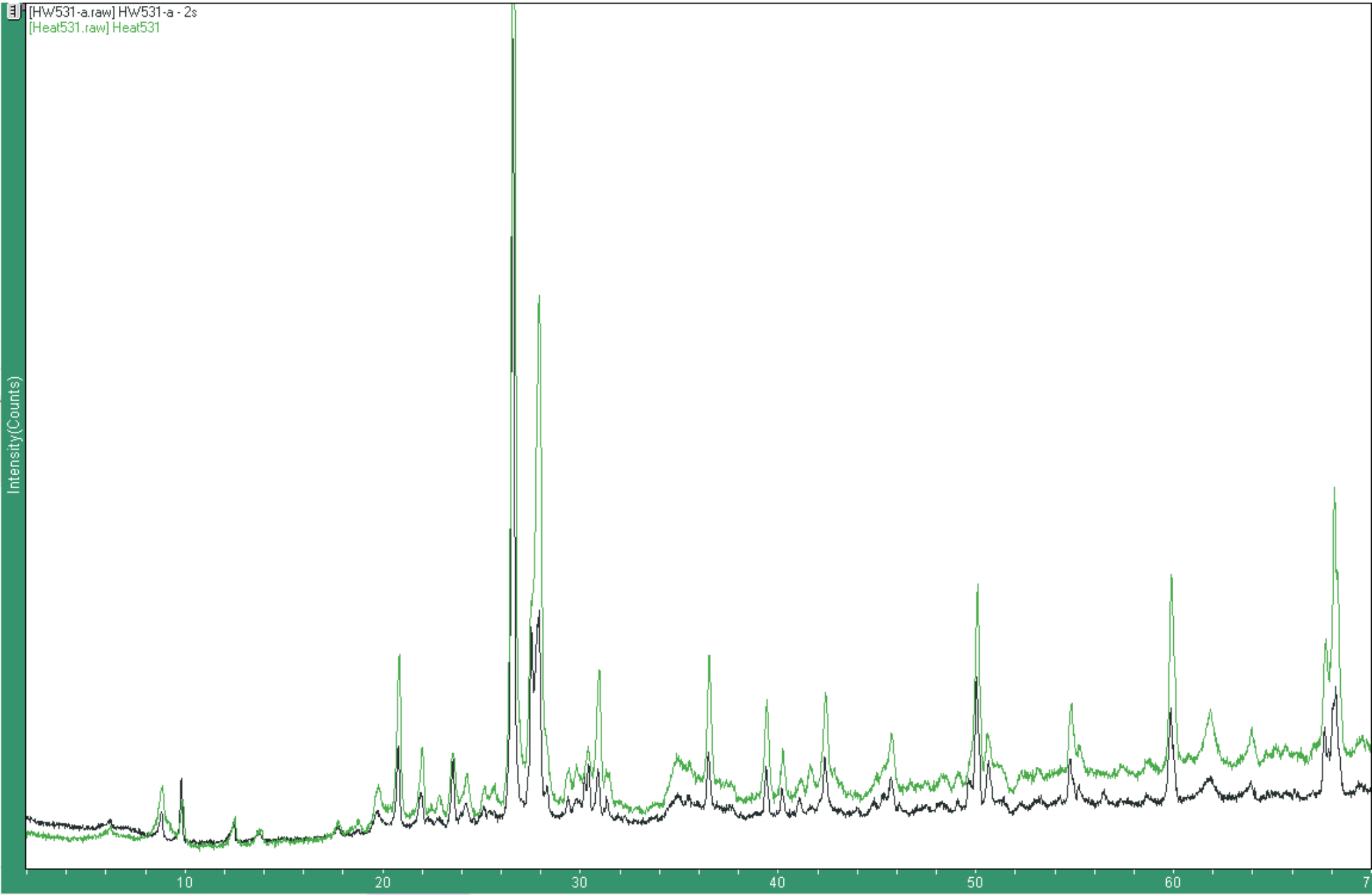
[HW531-a.raw] HW531-a - 2s
[Heat531.raw] Heat531
Intensity(Counts)
10
20
30
40
50
60
7

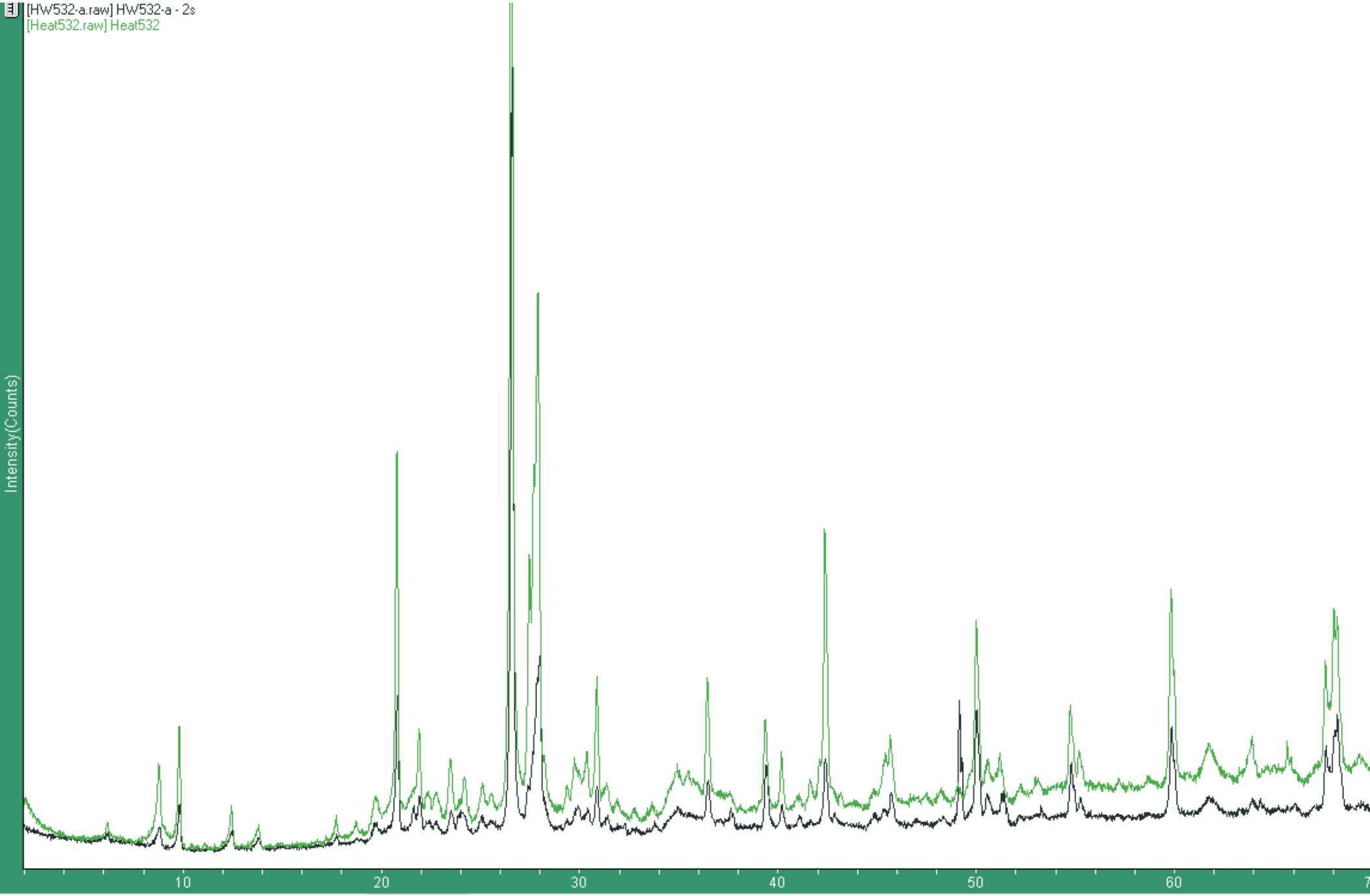
[HW532-a.raw] HW532-a - 2s
[Heat532.raw] Heat532
Intensity(Counts)
10
20
30
40
50
60

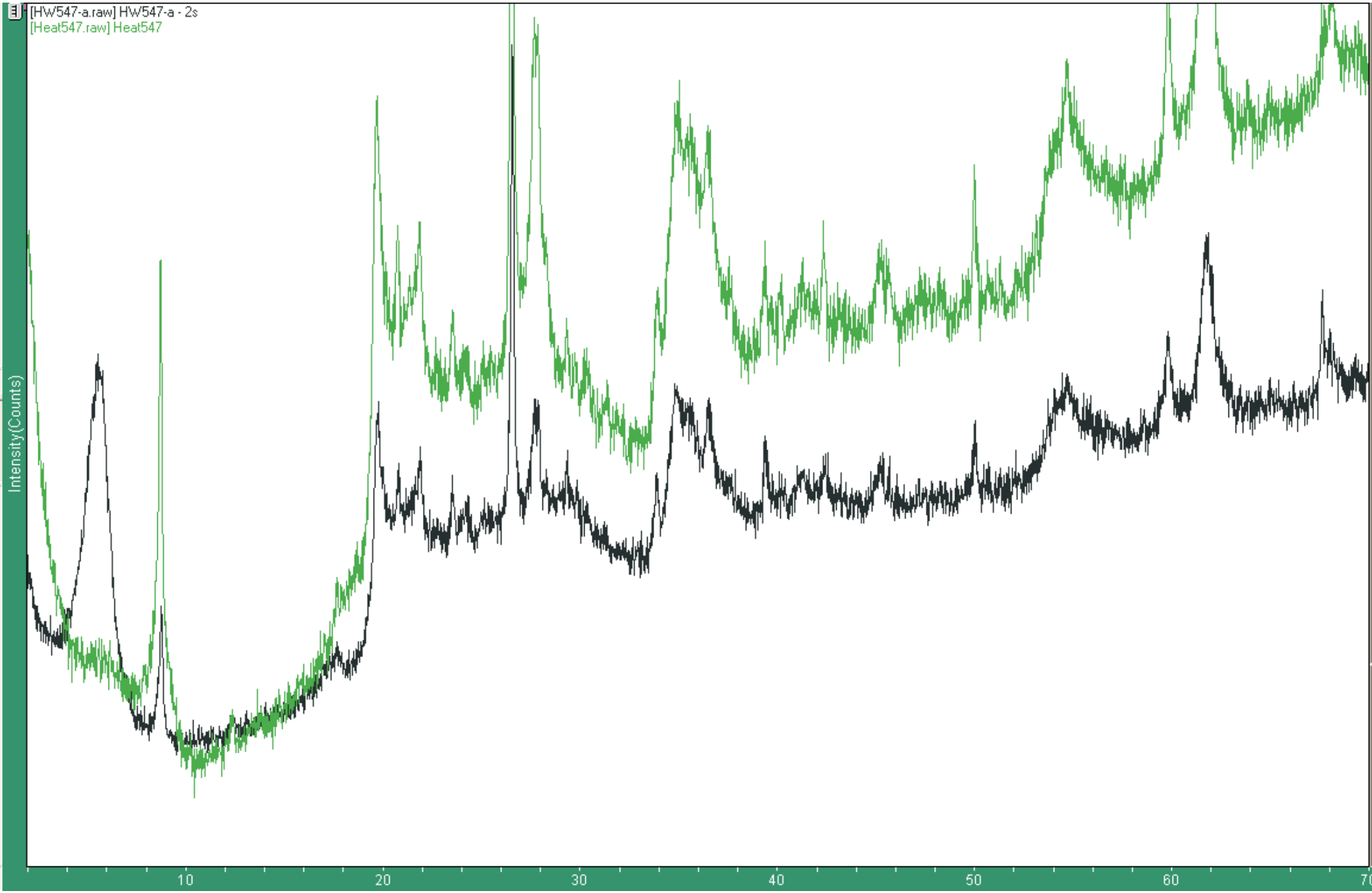
[HW547-a.raw] HW547-a - 2s
[Heat547.raw] Heat547
Intensity(Counts)
10
20
30
40
50
60
70

RAW AND GLYCOL TREATED X-RAY DIFFRACTOGRAMS

HW518 Comparison of dry run and glycol saturated: Untreated peak highlighted at 15.675 Angstroms.

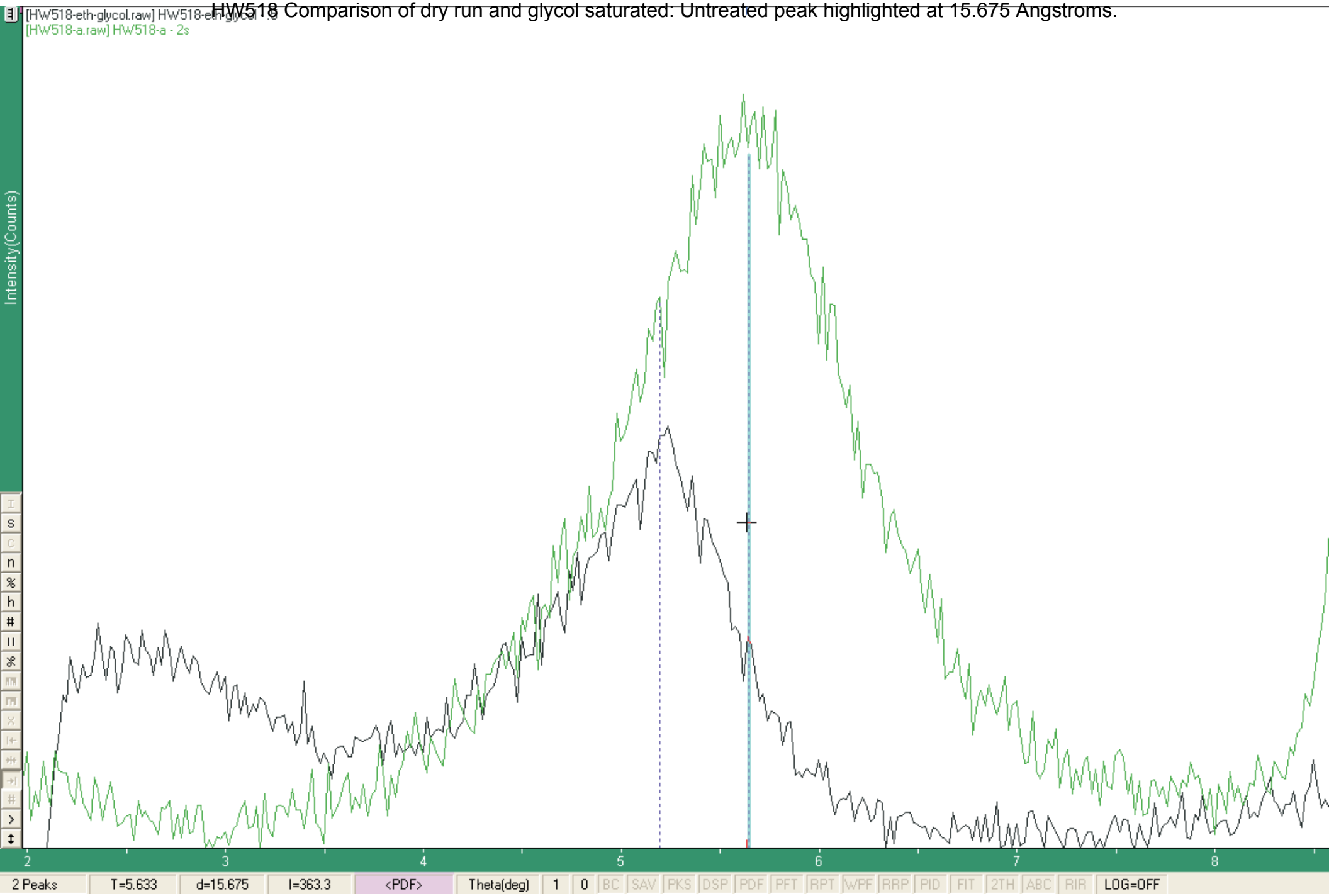

HW518 Comparison of dry run and glycol saturated: Treated peak highlighted at 17.018 Angstroms.

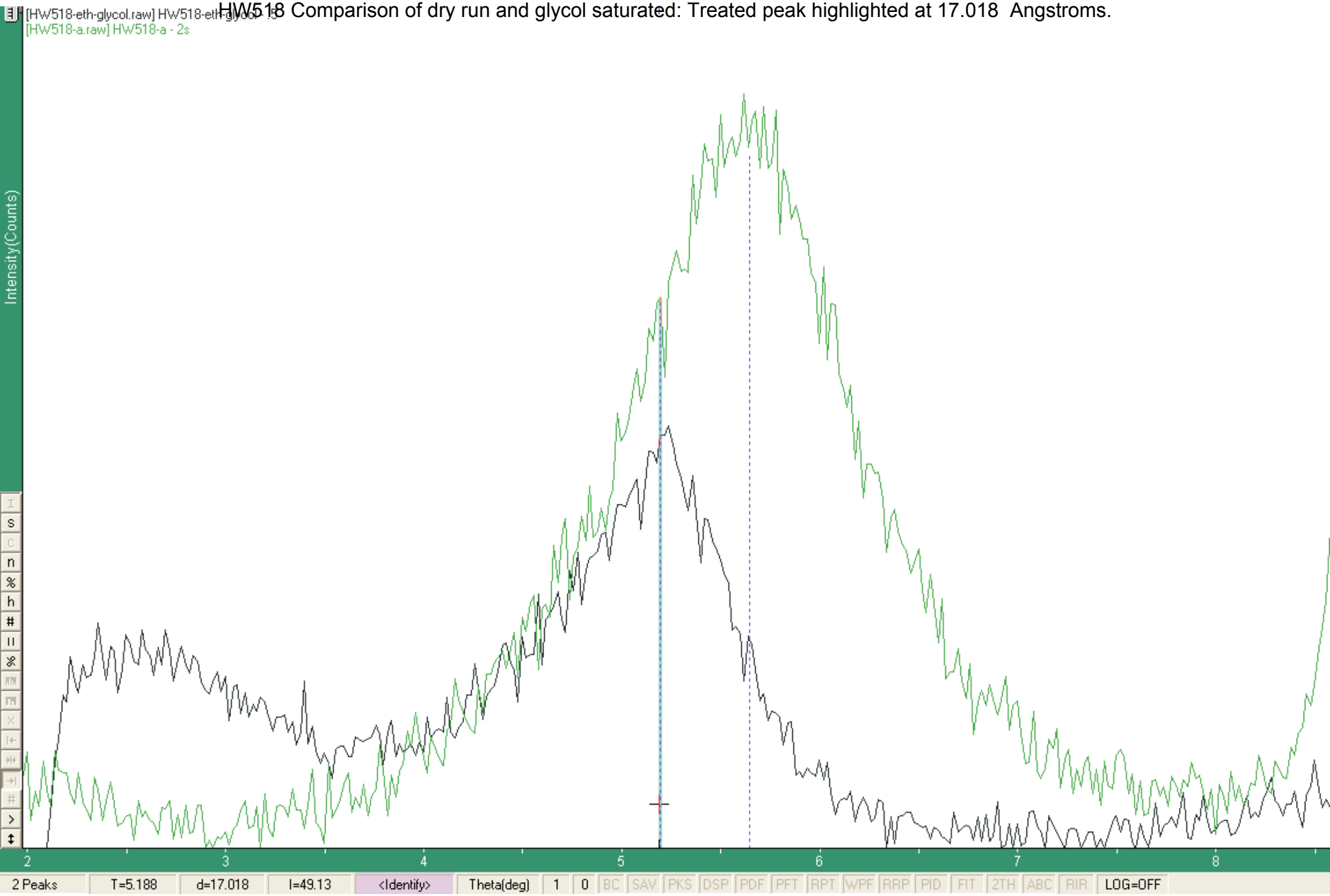

HW522 Comparison of dry run and glycol saturated: Untreated peak highlighted at 15.207 Angstroms.

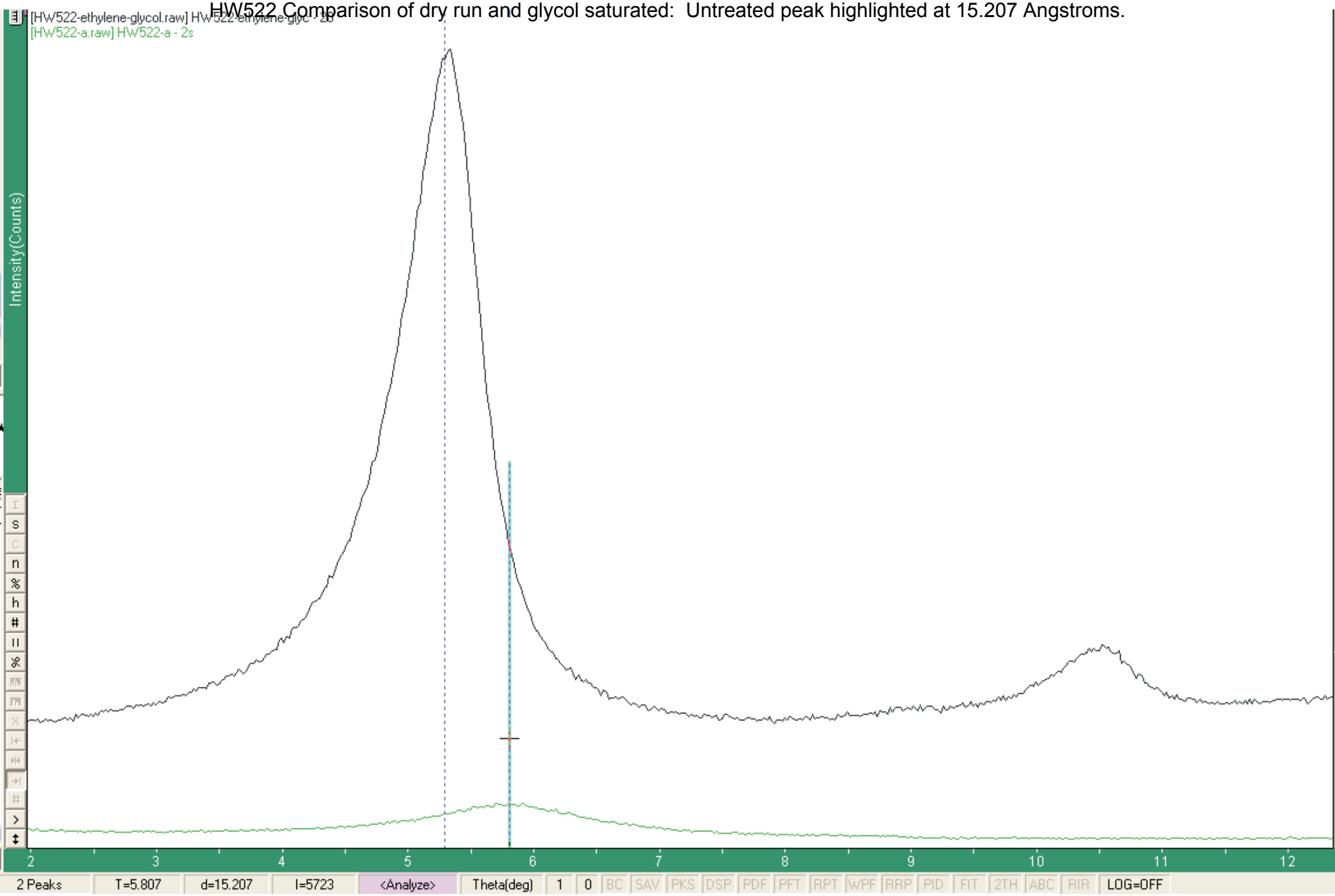

Comparison of dry run and glycol saturated: Treated peak at 16.715 Angstroms.

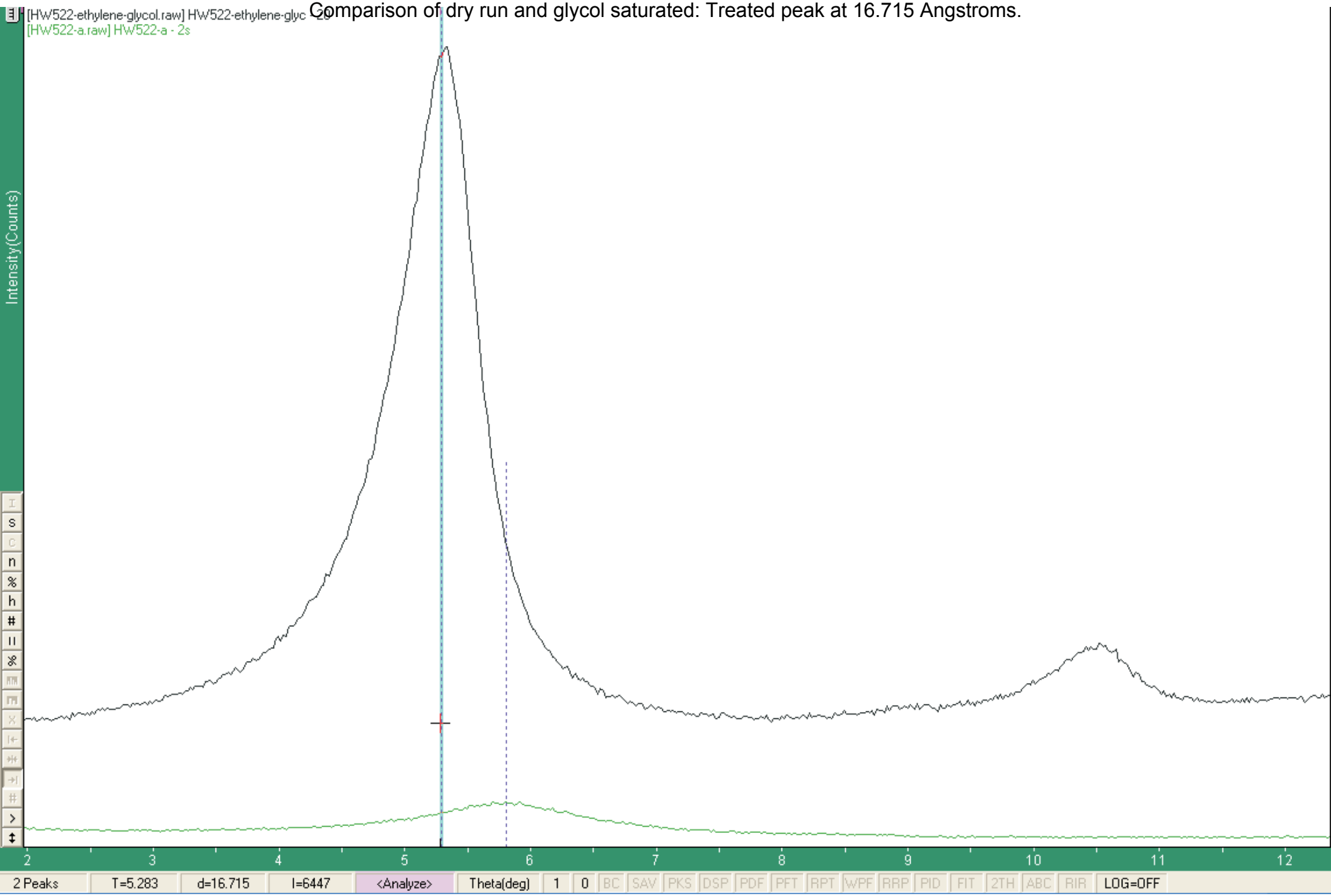

HW547 Comparison of dry run and ethylene glycol: Untreated peak highlighted at 15.837 Angstroms.

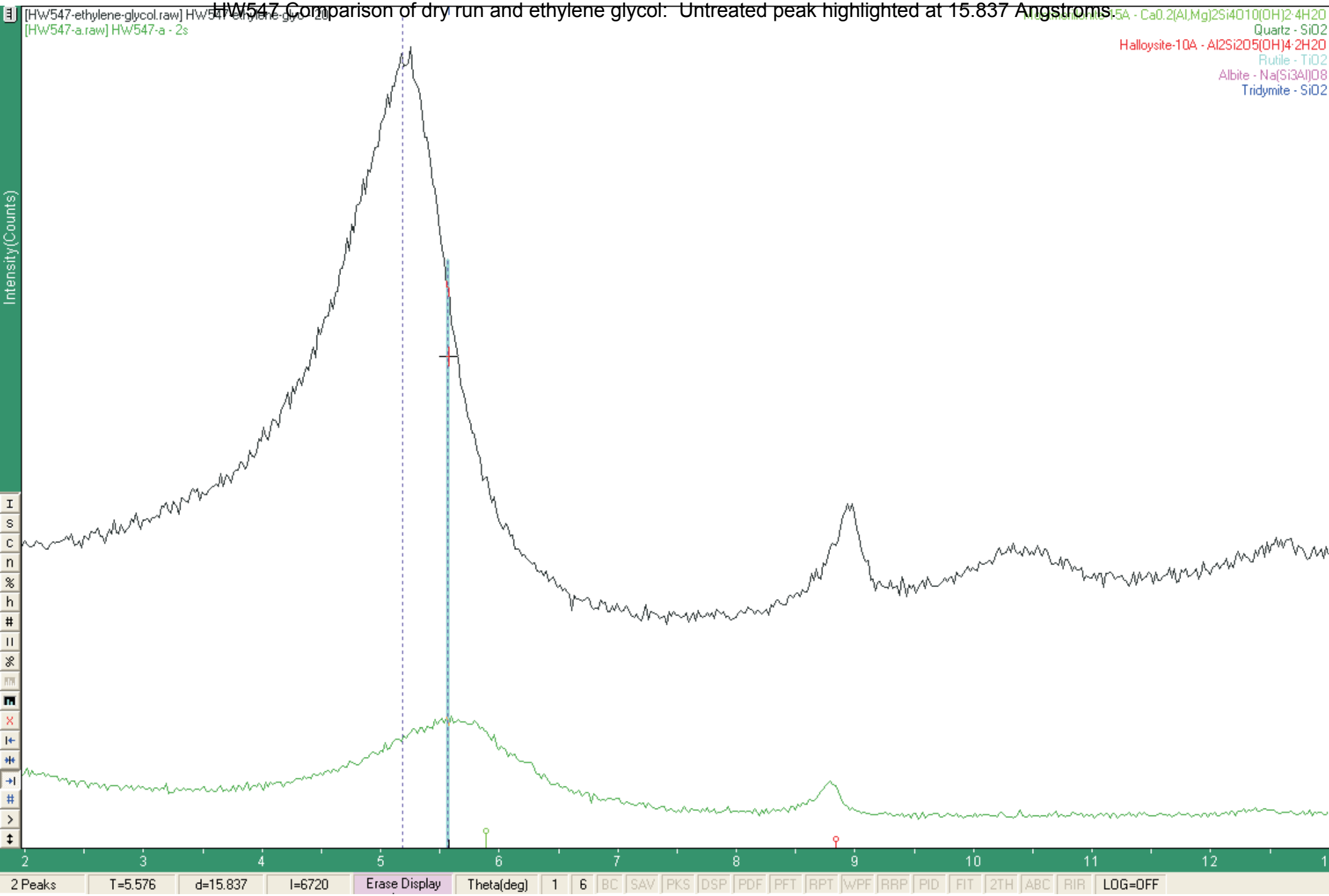

Comparison of dry run and glycol saturated: Treated peak at 17 Angstroms.

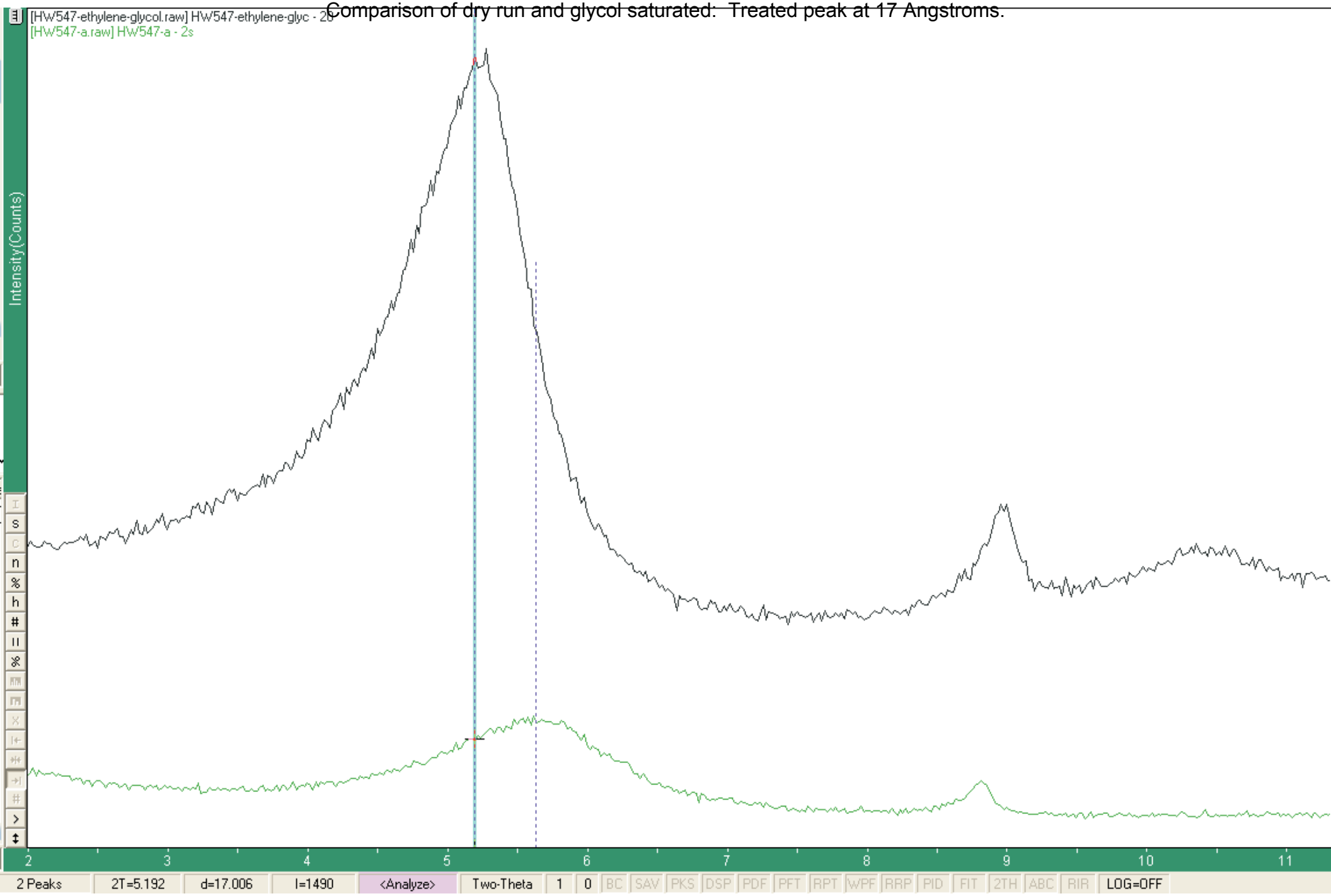

RAW X-RAY DIFFRACTOGRAMS AND MINERAL CALCULATIONS

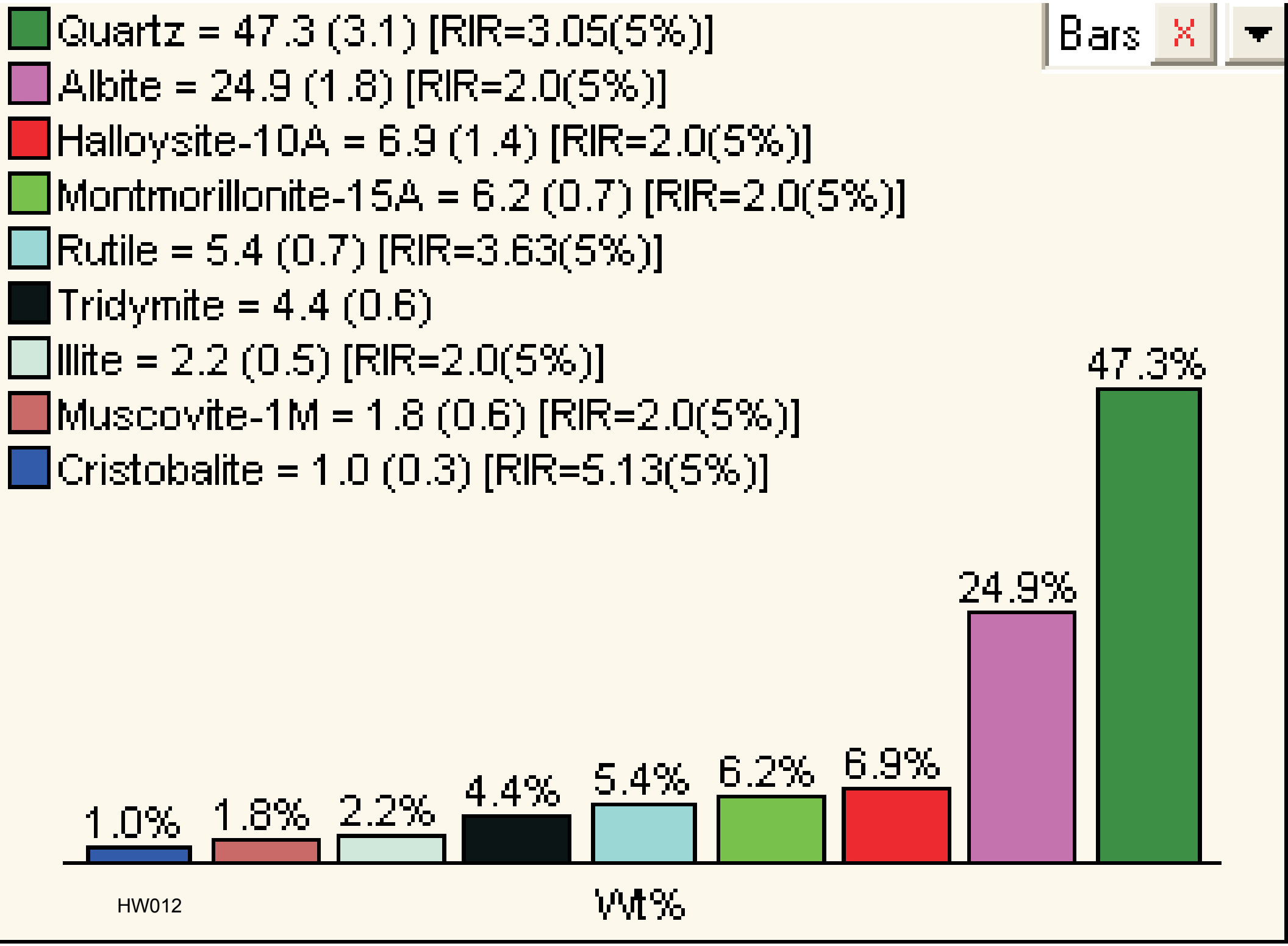
Quartz = 47.3 (3.1) [RIR=3.05(5%)]
Albite = 24.9 (1.8) [RIR=2.0(5%)]
Halloysite-10A = 6.9 (1.4) [RIR=2.0(5%)]
Montmorillonite-15A = 6.2 (0.7) [RIR=2.0(5%)]
Rutile = 5.4 (0.7) [RIR=3.63(5%)]
Tridymite = 4.4 (0.6)
Illite = 2.2 (0.5) [RIR=2.0(5%)]
Muscovite-1M = 1.8 (0.6) [RIR=2.0(5%)]
Cristobalite = 1.0 (0.3) [RIR=5.13(5%)]
Bars
1.0%
1.8%
2.2%
4.4%
5.4%
6.2%
6.9%
24.9%
47.3%
HW012
Wt%

HW012

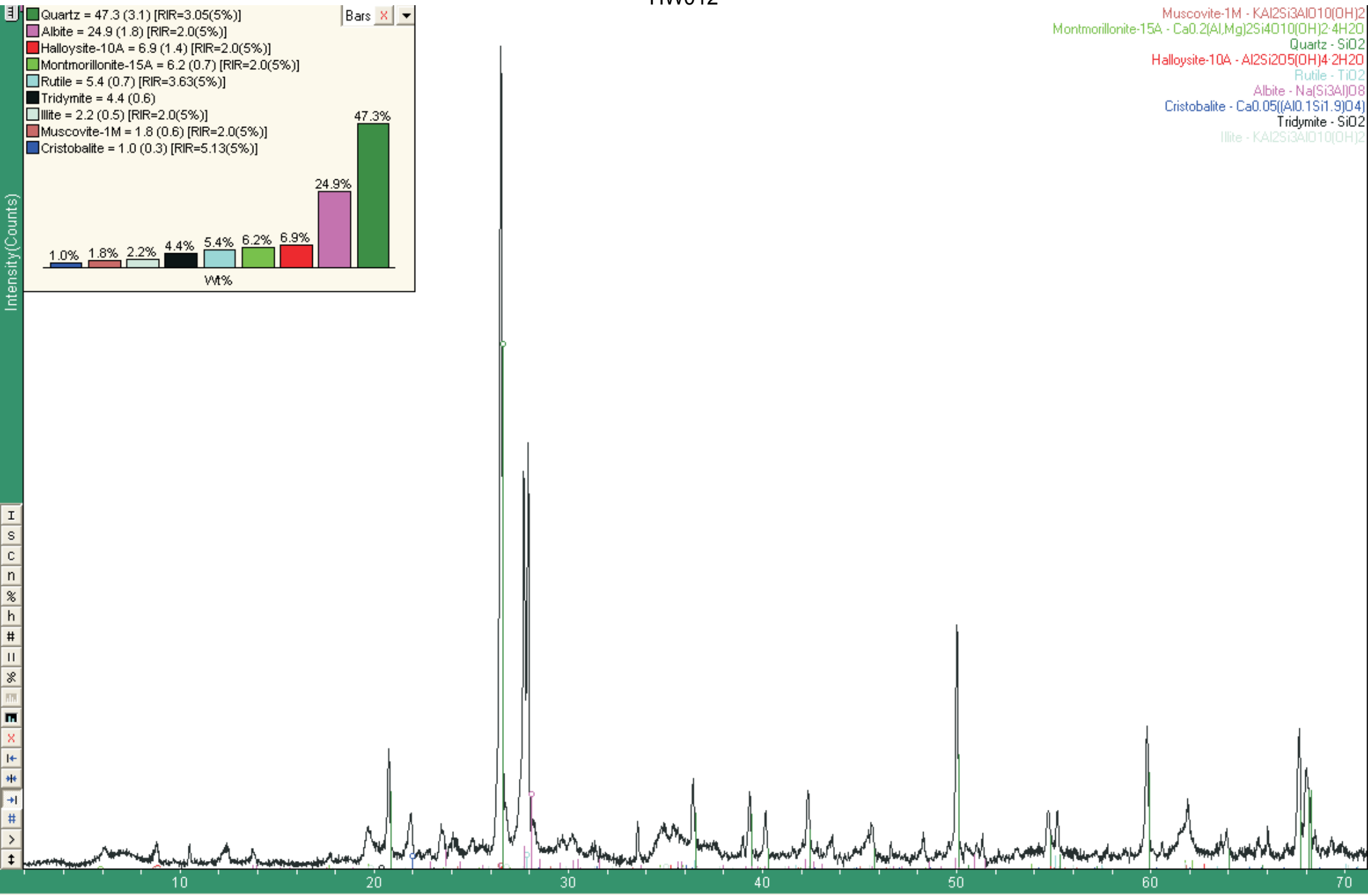
Quartz = 47.3 (3.1) [RIR=3.05(5%)]
Albite = 24.9 (1.8) [RIR=2.0(5%)]
Halloysite-10A = 6.9 (1.4) [RIR=2.0(5%)]
Montmorillonite-15A = 6.2 (0.7) [RIR=2.0(5%)]
Rutile = 5.4 (0.7) [RIR=3.63(5%)]
Tridymite = 4.4 (0.6)
Illite = 2.2 (0.5) [RIR=2.0(5%)]
Muscovite-1M = 1.8 (0.6) [RIR=2.0(5%)]
Cristobalite = 1.0 (0.3) [RIR=5.13(5%)]
Bars
1.0%
1.8%
2.2%
4.4%
5.4%
6.2%
6.9%
24.9%
47.3%
Wt%
Muscovite-1M - KAl2Si3AlO10(OH)2
Montmorillonite-15A - Ca0.2(Al,Mg)2Si4O10(OH)2·4H2O
Quartz - SiO2
Halloysite-10A - Al2Si2O5(OH)4·2H2O
Rutile - TiO2
Albite - Na(Si3Al)O8
Cristobalite - Ca0.05[(Al0.1Si1.9)O4]
Tridymite - SiO2
Illite - KAl2Si3AlO10(OH)2
Intensity(Counts)
10
20
30
40
50
60
70

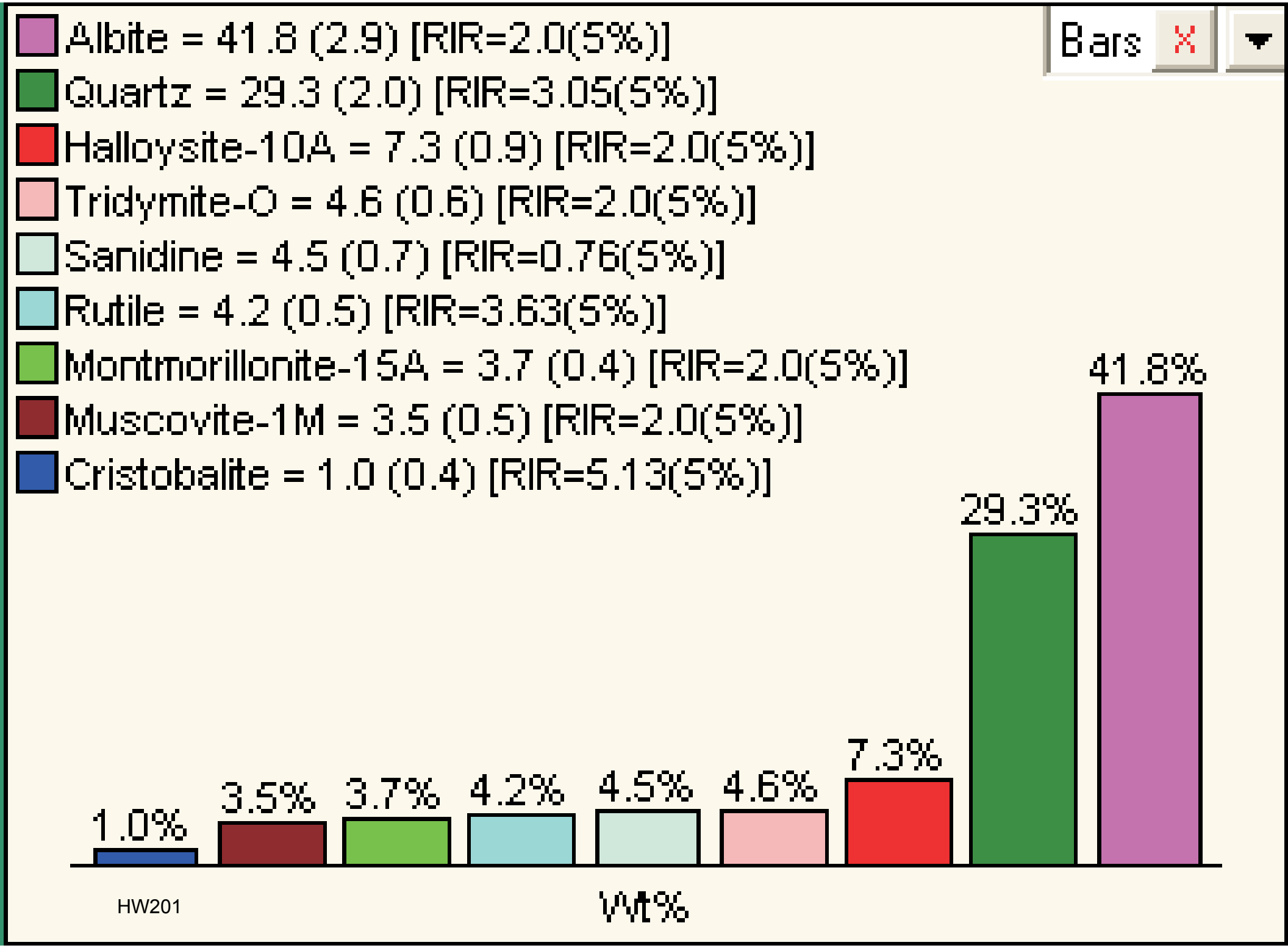
Albite = 41.8 (2.9) [RIR=2.0(5%)]
Quartz = 29.3 (2.0) [RIR=3.05(5%)]
Halloysite-10A = 7.3 (0.9) [RIR=2.0(5%)]
Tridymite-O = 4.6 (0.6) [RIR=2.0(5%)]
Sanidine = 4.5 (0.7) [RIR=0.76(5%)]
Rutile = 4.2 (0.5) [RIR=3.63(5%)]
Montmorillonite-15A = 3.7 (0.4) [RIR=2.0(5%)]
Muscovite-1M = 3.5 (0.5) [RIR=2.0(5%)]
Cristobalite = 1.0 (0.4) [RIR=5.13(5%)]
Bars
1.0%
3.5%
3.7%
4.2%
4.5%
4.6%
7.3%
29.3%
41.8%
HW201
Wt%

HW201

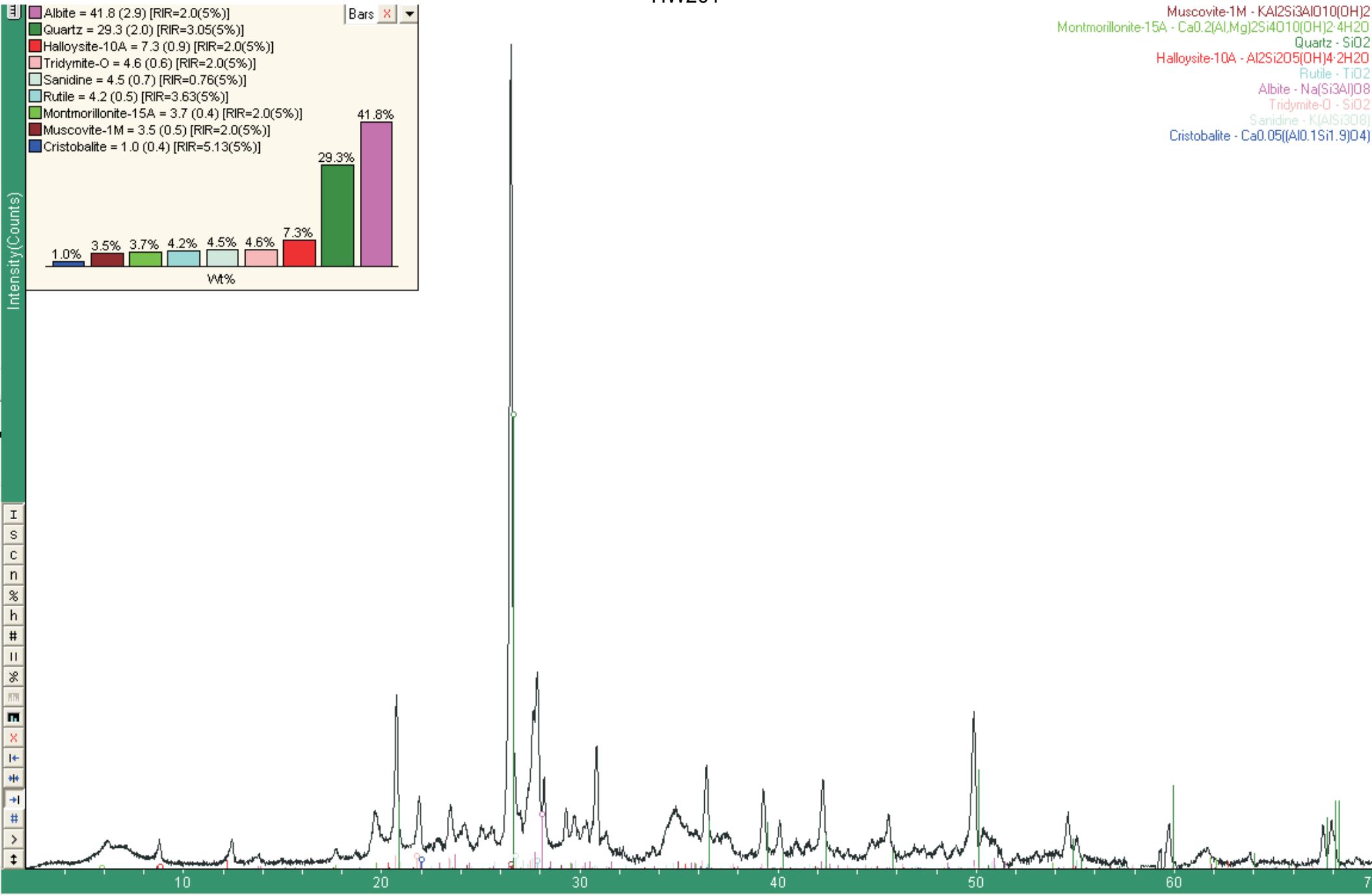
Albite = 41.8 (2.9) [RIR=2.0(5%)]
Quartz = 29.3 (2.0) [RIR=3.05(5%)]
Halloysite-10A = 7.3 (0.9) [RIR=2.0(5%)]
Tridymite-O = 4.6 (0.6) [RIR=2.0(5%)]
Sanidine = 4.5 (0.7) [RIR=0.76(5%)]
Rutile = 4.2 (0.5) [RIR=3.63(5%)]
Montmorillonite-15A = 3.7 (0.4) [RIR=2.0(5%)]
Muscovite-1M = 3.5 (0.5) [RIR=2.0(5%)]
Cristobalite = 1.0 (0.4) [RIR=5.13(5%)]
Bars
1.0%
3.5%
3.7%
4.2%
4.5%
4.6%
7.3%
29.3%
41.8%
Wt%
Muscovite-1M - KAl2Si3AlO10(OH)2
Montmorillonite-15A - Ca0.2(Al,Mg)2Si4O10(OH)2·4H2O
Quartz - SiO2
Halloysite-10A - Al2Si2O5(OH)4·2H2O
Rutile - TiO2
Albite - Na(Si3Al)O8
Tridymite-O - SiO2
Sanidine - K(AlSi3O8)
Cristobalite - Ca0.05((Al0.1Si1.9)O4)
Intensity(Counts)
10
20
30
40
50
60

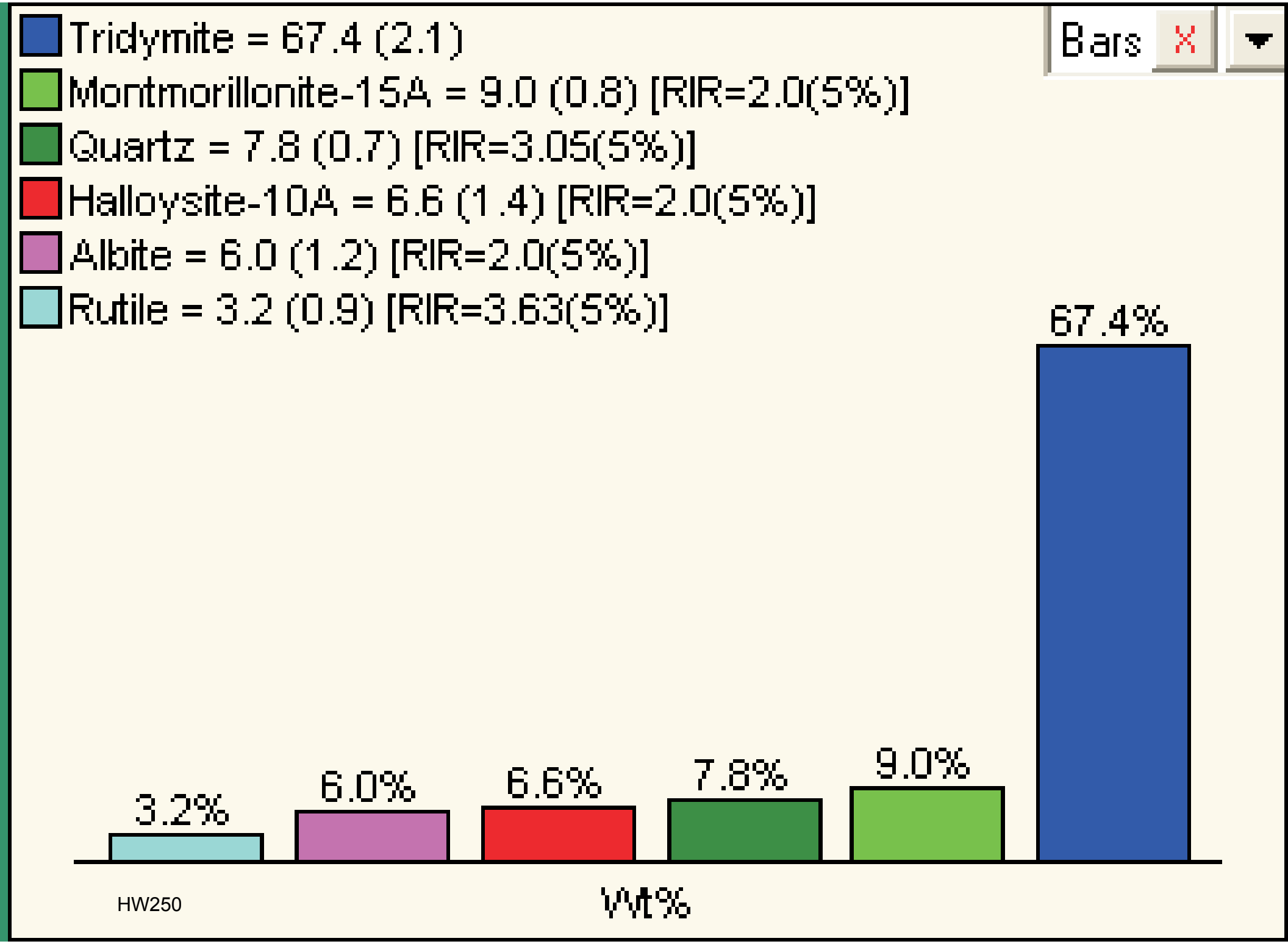
Tridymite = 67.4 (2.1)
Montmorillonite-15A = 9.0 (0.8) [RIR=2.0(5%)]
Quartz = 7.8 (0.7) [RIR=3.05(5%)]
Halloysite-10A = 6.6 (1.4) [RIR=2.0(5%)]
Albite = 6.0 (1.2) [RIR=2.0(5%)]
Rutile = 3.2 (0.9) [RIR=3.63(5%)]
Bars
3.2%
6.0%
6.6%
7.8%
9.0%
67.4%
HW250
Wt%

HW250

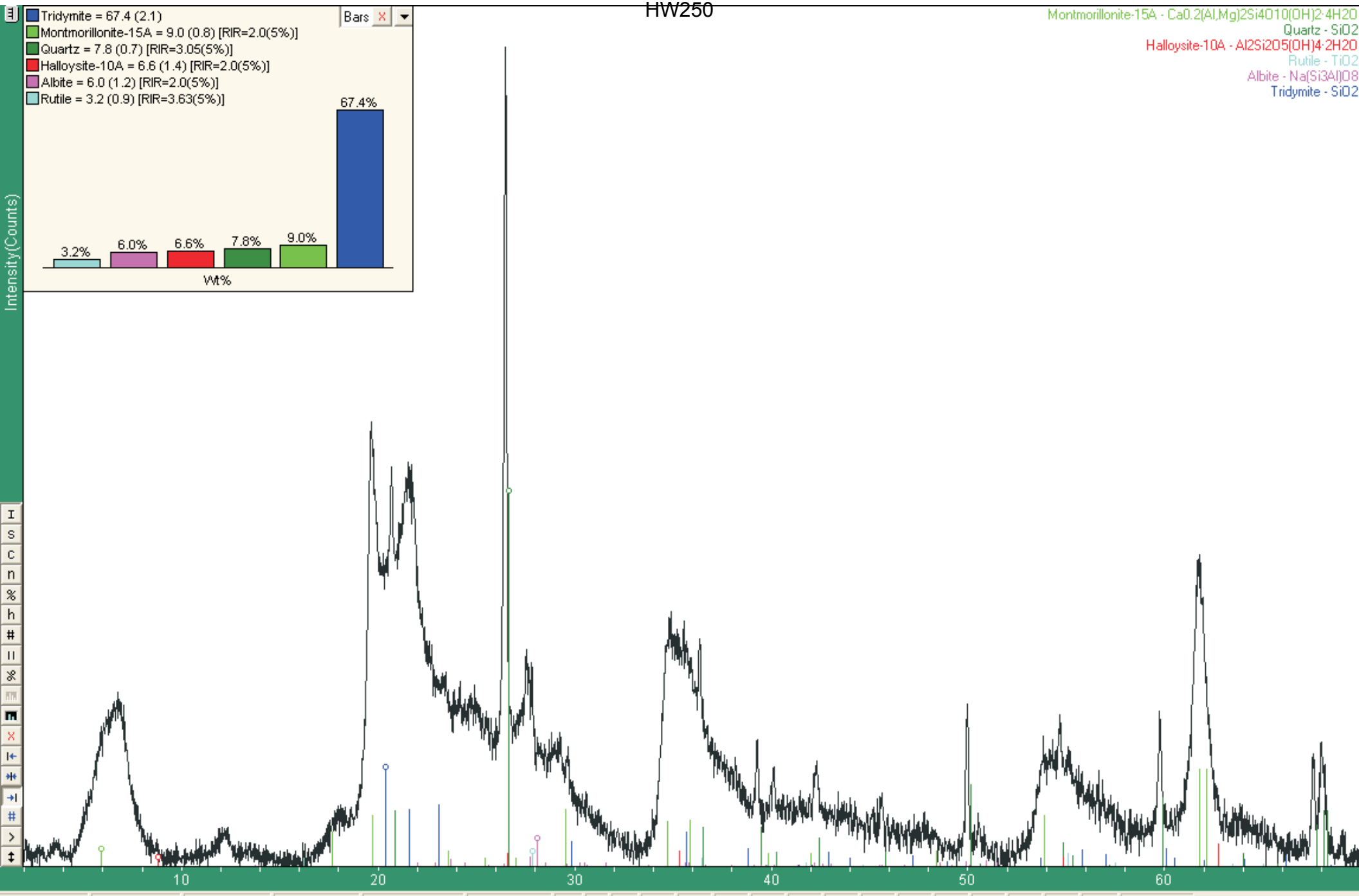

0 Peaks | T=16.267 | d=5.4445 | I=5483 | Save | Theta(deg) | 0 | 6 | BC | SAV | PKS | DSP | PDF | PFT | RPT | WPF | RRP | PID | FIT | 2TH | ABC | RIR | LOG=OFF

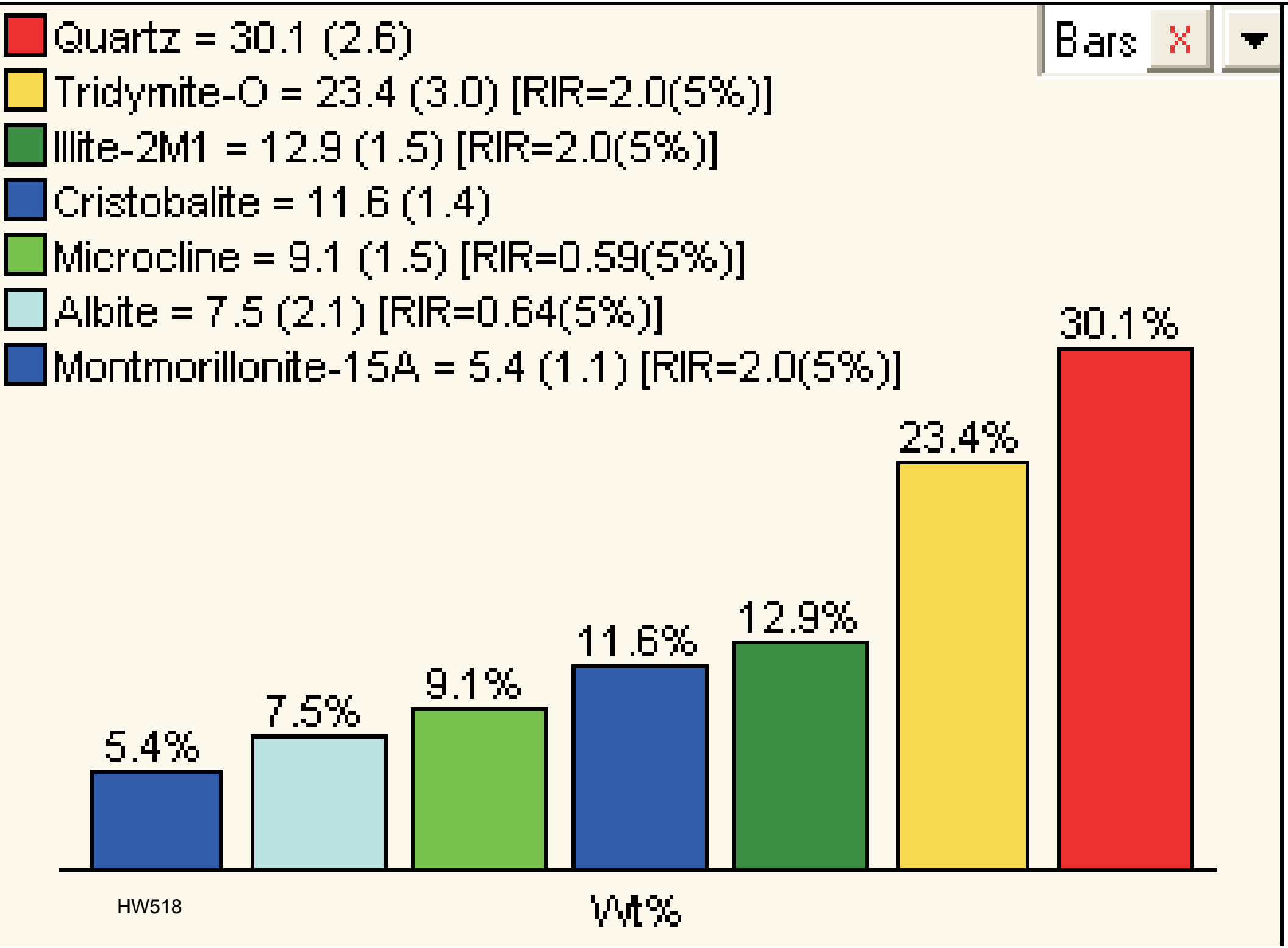
Quartz = 30.1 (2.6)
Tridymite-O = 23.4 (3.0) [RIR=2.0(5%)]
Illite-2M1 = 12.9 (1.5) [RIR=2.0(5%)]
Cristobalite = 11.6 (1.4)
Microcline = 9.1 (1.5) [RIR=0.59(5%)]
Albite = 7.5 (2.1) [RIR=0.64(5%)]
Montmorillonite-15A = 5.4 (1.1) [RIR=2.0(5%)]
Bars
5.4%
7.5%
9.1%
11.6%
12.9%
23.4%
30.1%
HW518
Wt%

HW518

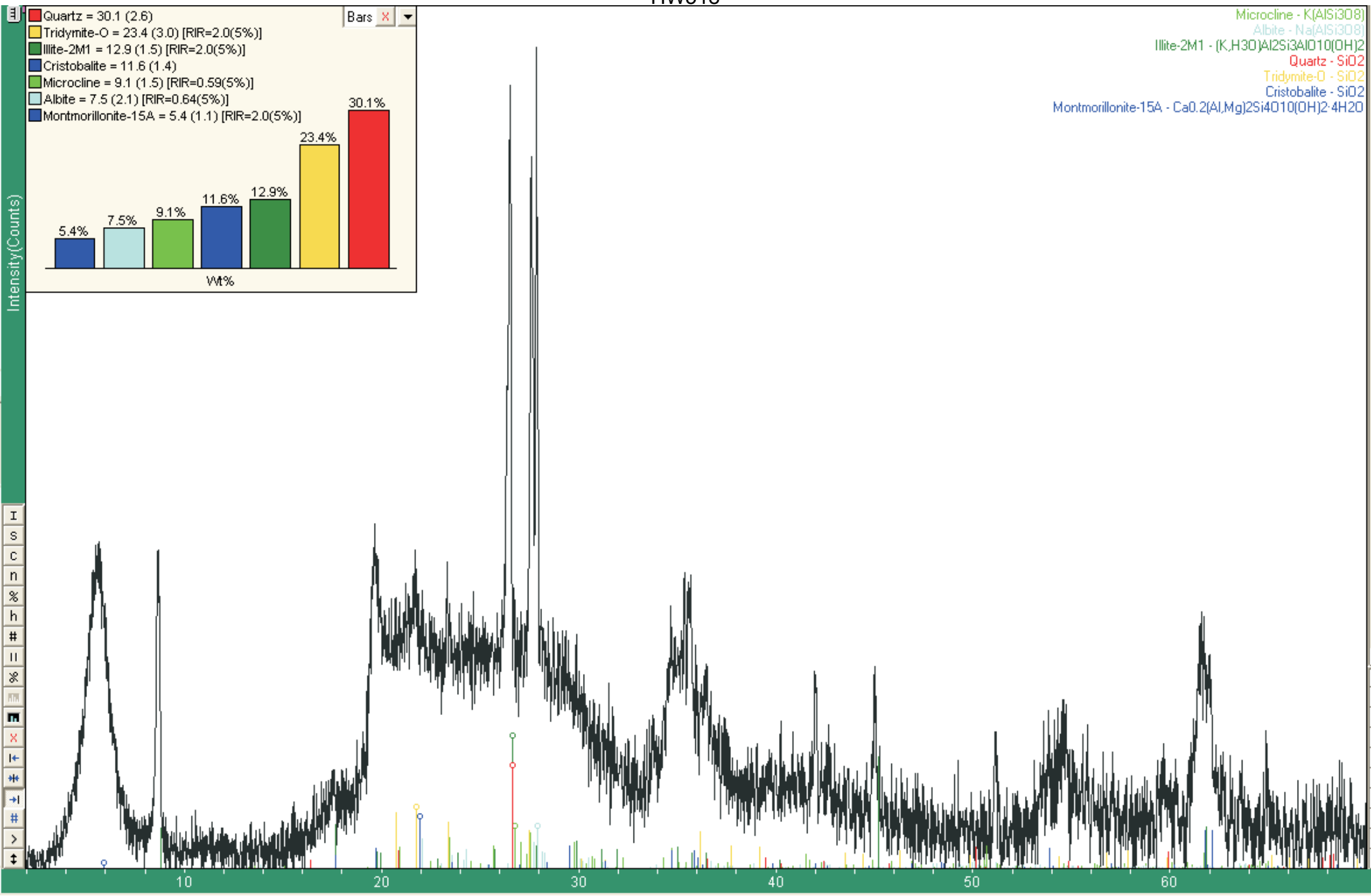
Quartz = 30.1 (2.6)
Tridymite-O = 23.4 (3.0) [RIR=2.0(5%)]
Illite-2M1 = 12.9 (1.5) [RIR=2.0(5%)]
Cristobalite = 11.6 (1.4)
Microcline = 9.1 (1.5) [RIR=0.59(5%)]
Albite = 7.5 (2.1) [RIR=0.64(5%)]
Montmorillonite-15A = 5.4 (1.1) [RIR=2.0(5%)]
Bars
5.4%
7.5%
9.1%
11.6%
12.9%
23.4%
30.1%
Wt%
Microcline - K(AlSi3O8)
Albite - Na(AlSi3O8)
Illite-2M1 - (K,H3O)Al2Si3AlO10(OH)2
Quartz - SiO2
Tridymite-O - SiO2
Cristobalite - SiO2
Montmorillonite-15A - Ca0.2(Al,Mg)2Si4O10(OH)2·4H2O
Intensity(Counts)
10
20
30
40
50
60

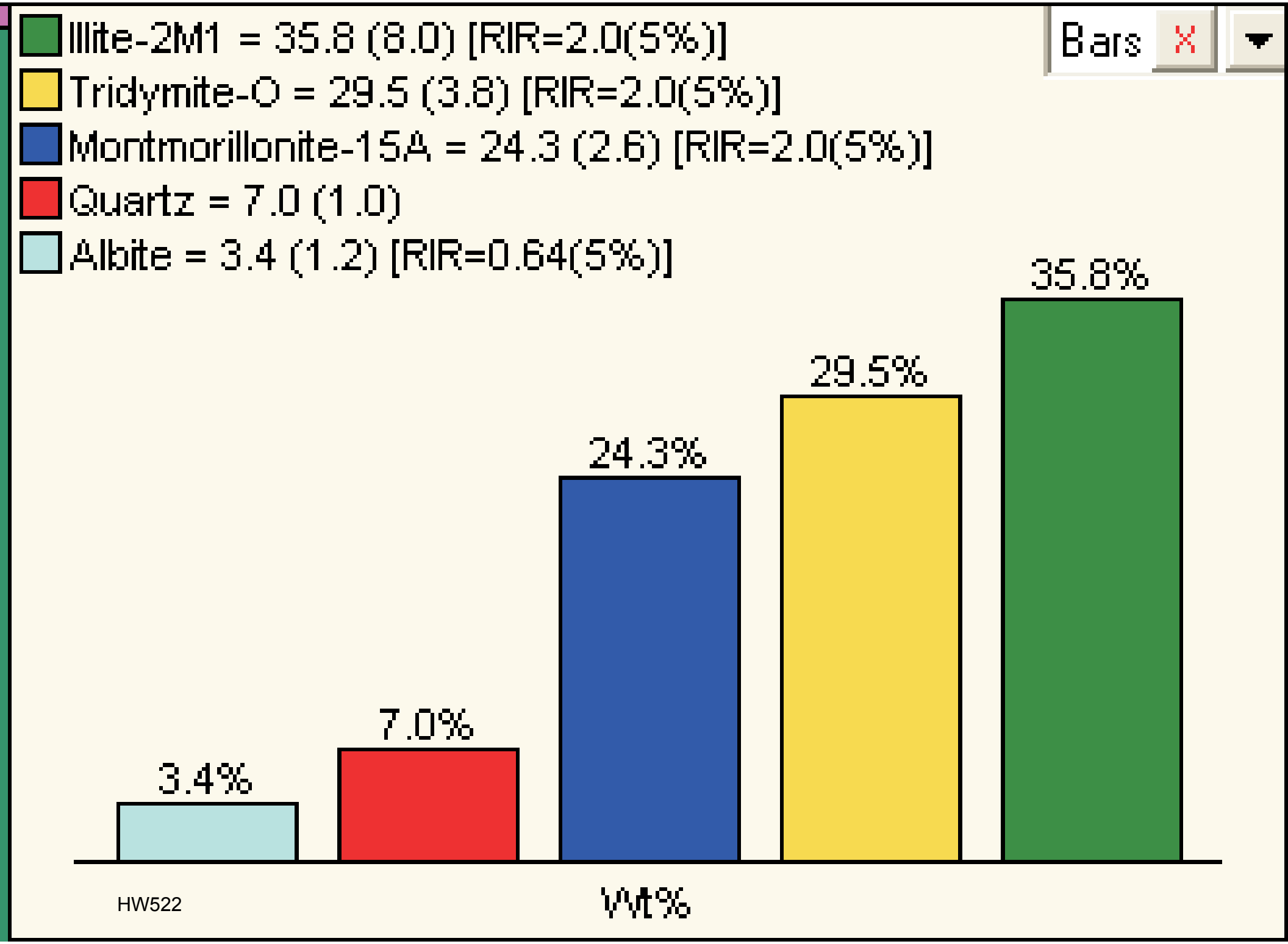
Illite-2M1 = 35.8 (8.0) [RIR=2.0(5%)]
Tridymite-O = 29.5 (3.8) [RIR=2.0(5%)]
Montmorillonite-15A = 24.3 (2.6) [RIR=2.0(5%)]
Quartz = 7.0 (1.0)
Albite = 3.4 (1.2) [RIR=0.64(5%)]
Bars
3.4%
7.0%
24.3%
29.5%
35.8%
HW522
Wt%

HW522

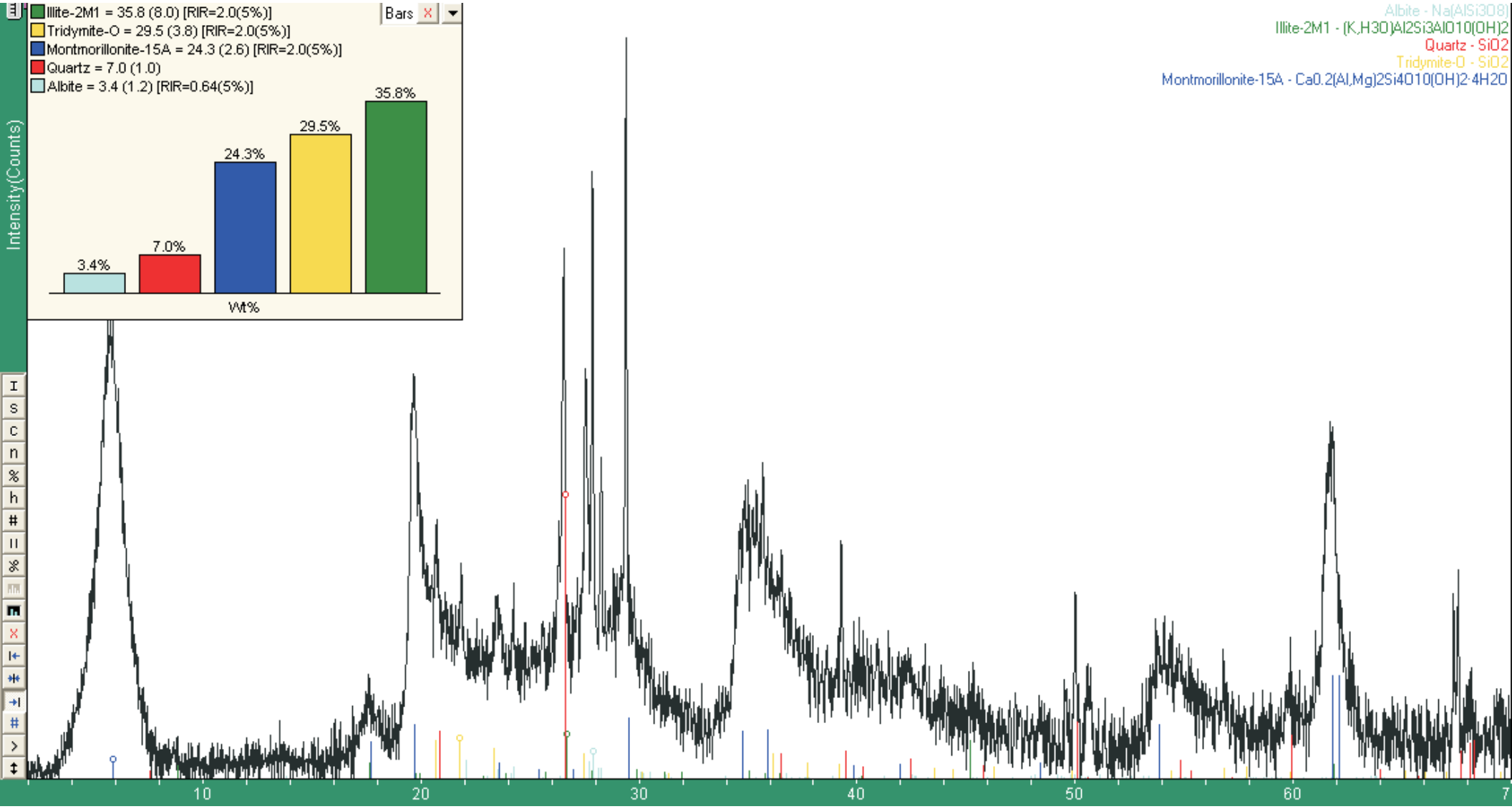
Illite-2M1 = 35.8 (8.0) [RIR=2.0(5%)]
Tridymite-O = 29.5 (3.8) [RIR=2.0(5%)]
Montmorillonite-15A = 24.3 (2.6) [RIR=2.0(5%)]
Quartz = 7.0 (1.0)
Albite = 3.4 (1.2) [RIR=0.64(5%)]
Bars
3.4%
7.0%
24.3%
29.5%
35.8%
Wt%
Intensity(Counts)
Albite - Na(AlSi3O8)
Illite-2M1 - (K,H3O)Al2Si3AlO10(OH)2
Quartz - SiO2
Tridymite-O - SiO2
Montmorillonite-15A - Ca0.2(Al,Mg)2Si4O10(OH)2·4H2O
10
20
30
40
50
60

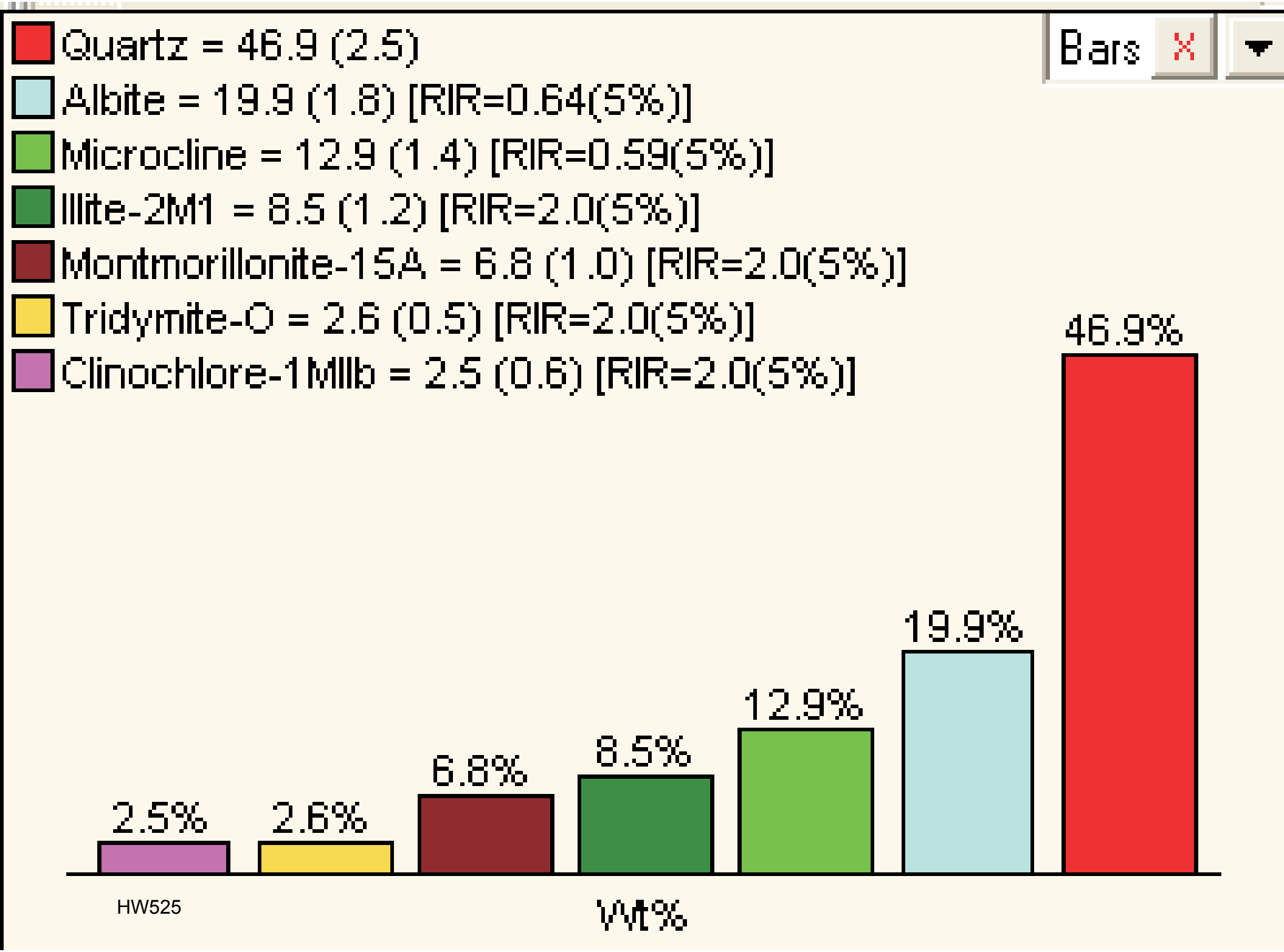
Quartz = 46.9 (2.5)
Albite = 19.9 (1.8) [RIR=0.64(5%)]
Microcline = 12.9 (1.4) [RIR=0.59(5%)]
Illite-2M1 = 8.5 (1.2) [RIR=2.0(5%)]
Montmorillonite-15A = 6.8 (1.0) [RIR=2.0(5%)]
Tridymite-O = 2.6 (0.5) [RIR=2.0(5%)]
Clinochlore-1MIIb = 2.5 (0.6) [RIR=2.0(5%)]
Bars
2.5%
2.6%
6.8%
8.5%
12.9%
19.9%
46.9%
HW525
Wt%

HW525

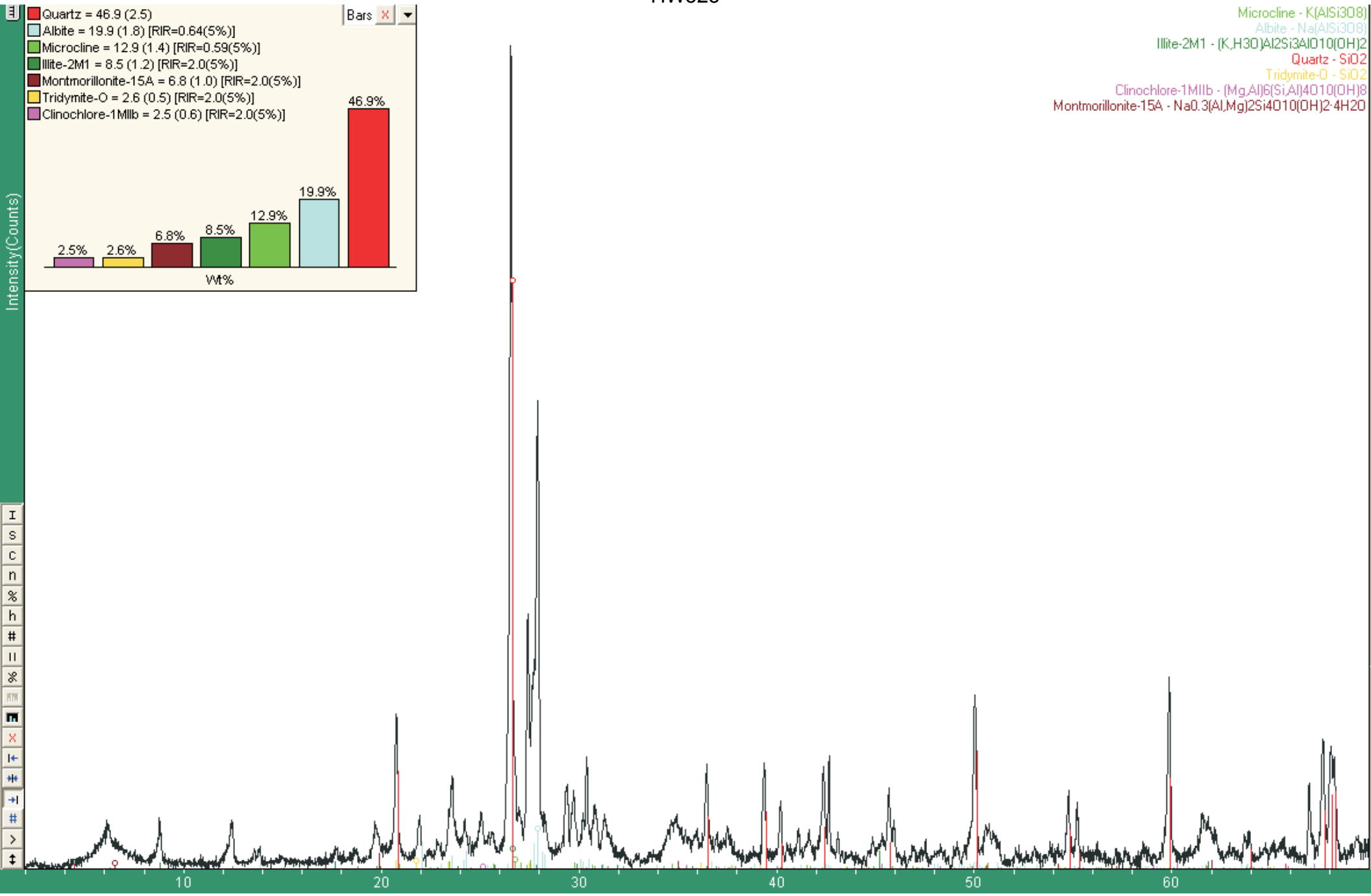
Quartz = 46.9 (2.5)
Albite = 19.9 (1.8) [RIR=0.64(5%)]
Microcline = 12.9 (1.4) [RIR=0.59(5%)]
Illite-2M1 = 8.5 (1.2) [RIR=2.0(5%)]
Montmorillonite-15A = 6.8 (1.0) [RIR=2.0(5%)]
Tridymite-O = 2.6 (0.5) [RIR=2.0(5%)]
Clinochlore-1MIIb = 2.5 (0.6) [RIR=2.0(5%)]
Bars
2.5%
2.6%
6.8%
8.5%
12.9%
19.9%
46.9%
Wt%
Microcline - K(AlSi3O8)
Albite - Na(AlSi3O8)
Illite-2M1 - (K,H3O)Al2Si3AlO10(OH)2
Quartz - SiO2
Tridymite-O - SiO2
Clinochlore-1MIIb - (Mg,Al)6(Si,Al)4O10(OH)8
Montmorillonite-15A - Na0.3(Al,Mg)2Si4O10(OH)2·4H2O
Intensity(Counts)
10
20
30
40
50
60

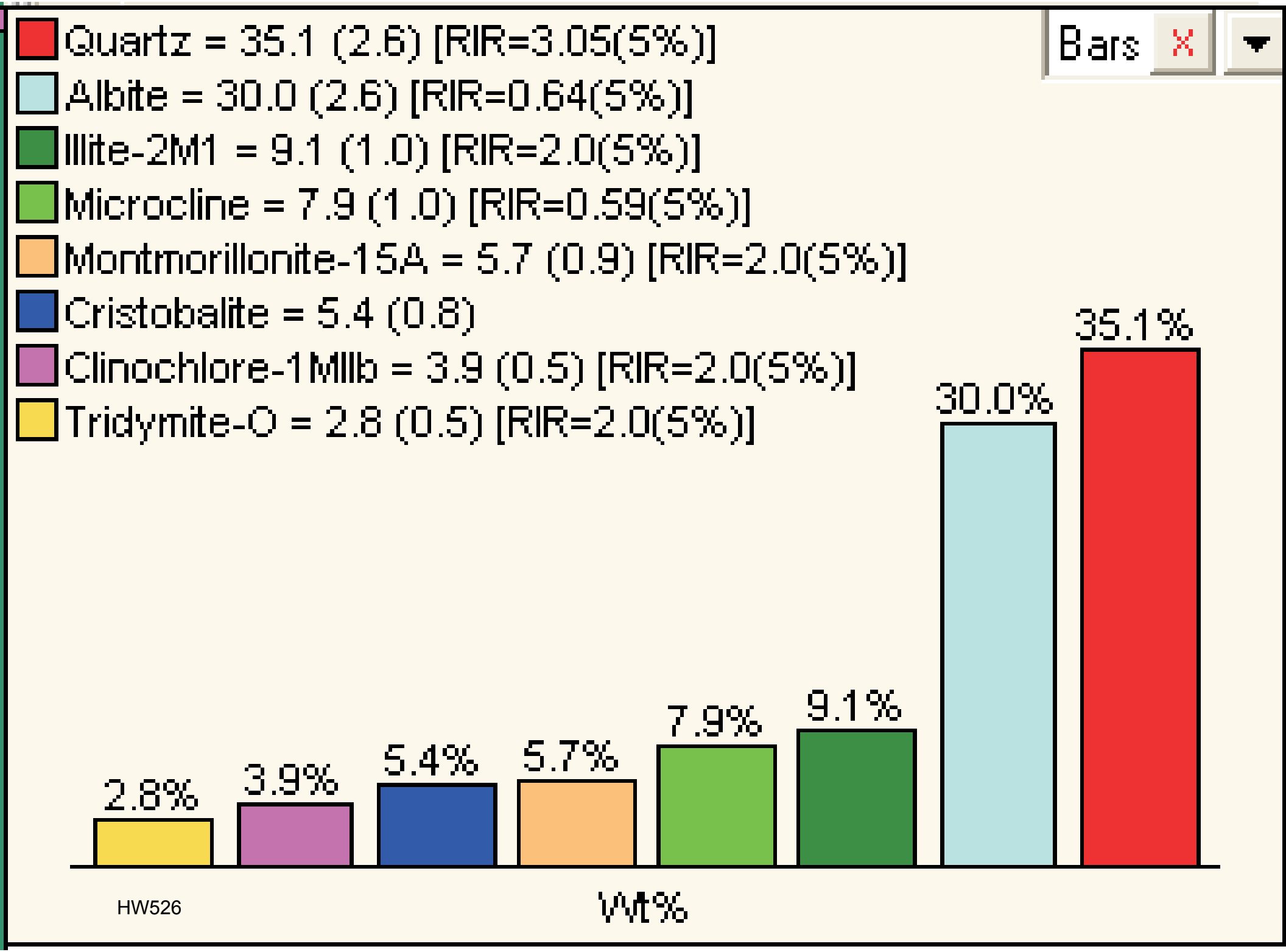
Quartz = 35.1 (2.6) [RIR=3.05(5%)]
Albite = 30.0 (2.6) [RIR=0.64(5%)]
Illite-2M1 = 9.1 (1.0) [RIR=2.0(5%)]
Microcline = 7.9 (1.0) [RIR=0.59(5%)]
Montmorillonite-15A = 5.7 (0.9) [RIR=2.0(5%)]
Cristobalite = 5.4 (0.8)
Clinochlore-1MIIb = 3.9 (0.5) [RIR=2.0(5%)]
Tridymite-O = 2.8 (0.5) [RIR=2.0(5%)]
Bars
2.8%
3.9%
5.4%
5.7%
7.9%
9.1%
30.0%
35.1%
HW526
Wt%

HW526

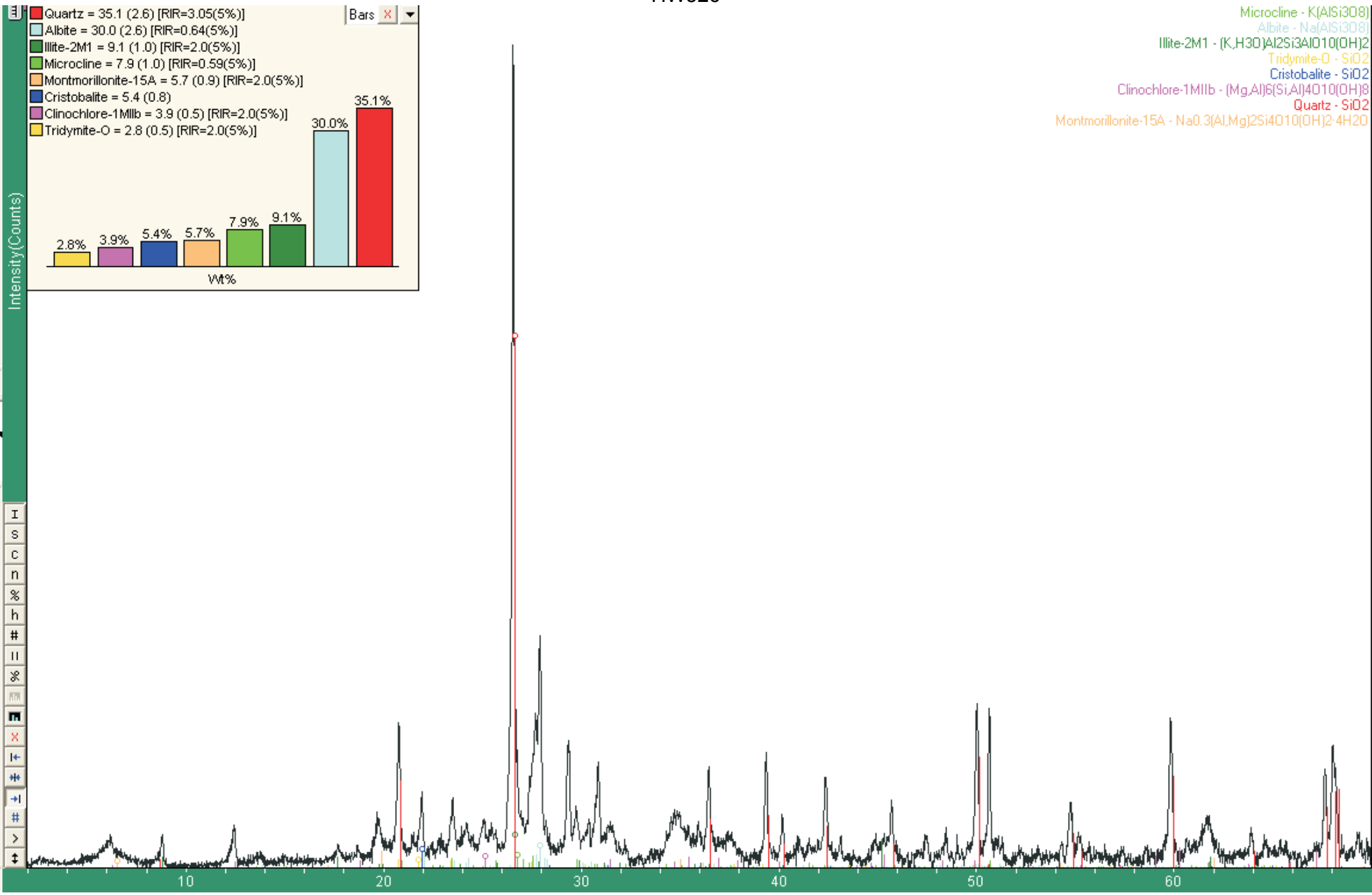
Quartz = 35.1 (2.6) [RIR=3.05(5%)]
Albite = 30.0 (2.6) [RIR=0.64(5%)]
Illite-2M1 = 9.1 (1.0) [RIR=2.0(5%)]
Microcline = 7.9 (1.0) [RIR=0.59(5%)]
Montmorillonite-15A = 5.7 (0.9) [RIR=2.0(5%)]
Cristobalite = 5.4 (0.8)
Clinochlore-1MIIb = 3.9 (0.5) [RIR=2.0(5%)]
Tridymite-O = 2.8 (0.5) [RIR=2.0(5%)]
Bars
2.8%
3.9%
5.4%
5.7%
7.9%
9.1%
30.0%
35.1%
Wt%
Microcline - K(AlSi3O8)
Albite - Na(AlSi3O8)
Illite-2M1 - (K,H3O)Al2Si3AlO10(OH)2
Tridymite-O - SiO2
Cristobalite - SiO2
Clinochlore-1MIIb - (Mg,Al)6(Si,Al)4O10(OH)8
Quartz - SiO2
Montmorillonite-15A - Na0.3(Al,Mg)2Si4O10(OH)2·4H2O
Intensity(Counts)
10
20
30
40
50
60

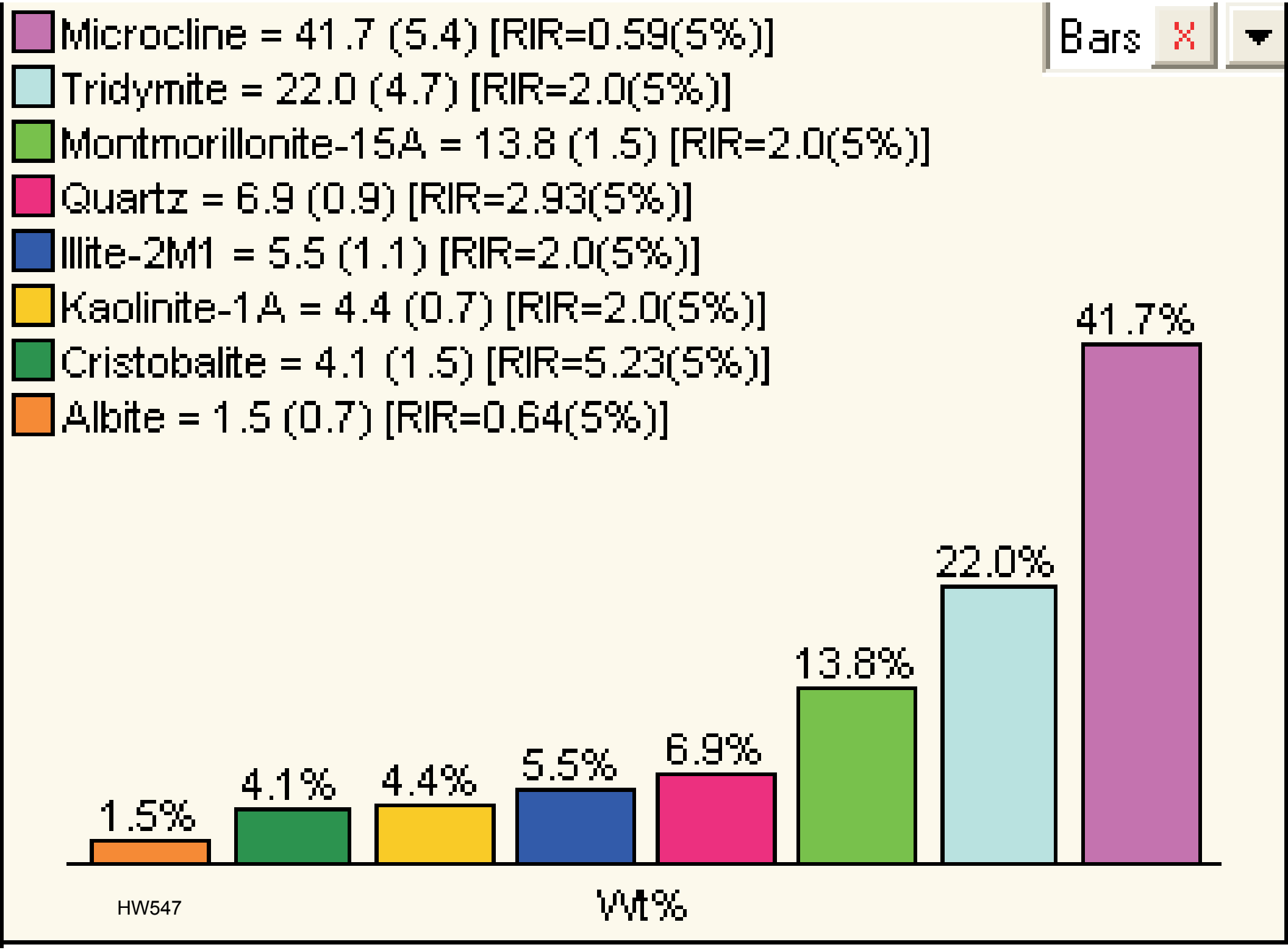
Microcline = 41.7 (5.4) [RIR=0.59(5%)]
Tridymite = 22.0 (4.7) [RIR=2.0(5%)]
Montmorillonite-15A = 13.8 (1.5) [RIR=2.0(5%)]
Quartz = 6.9 (0.9) [RIR=2.93(5%)]
Illite-2M1 = 5.5 (1.1) [RIR=2.0(5%)]
Kaolinite-1A = 4.4 (0.7) [RIR=2.0(5%)]
Cristobalite = 4.1 (1.5) [RIR=5.23(5%)]
Albite = 1.5 (0.7) [RIR=0.64(5%)]
Bars
X
1.5%
4.1%
4.4%
5.5%
6.9%
13.8%
22.0%
41.7%
HW547
Wt%

HW547

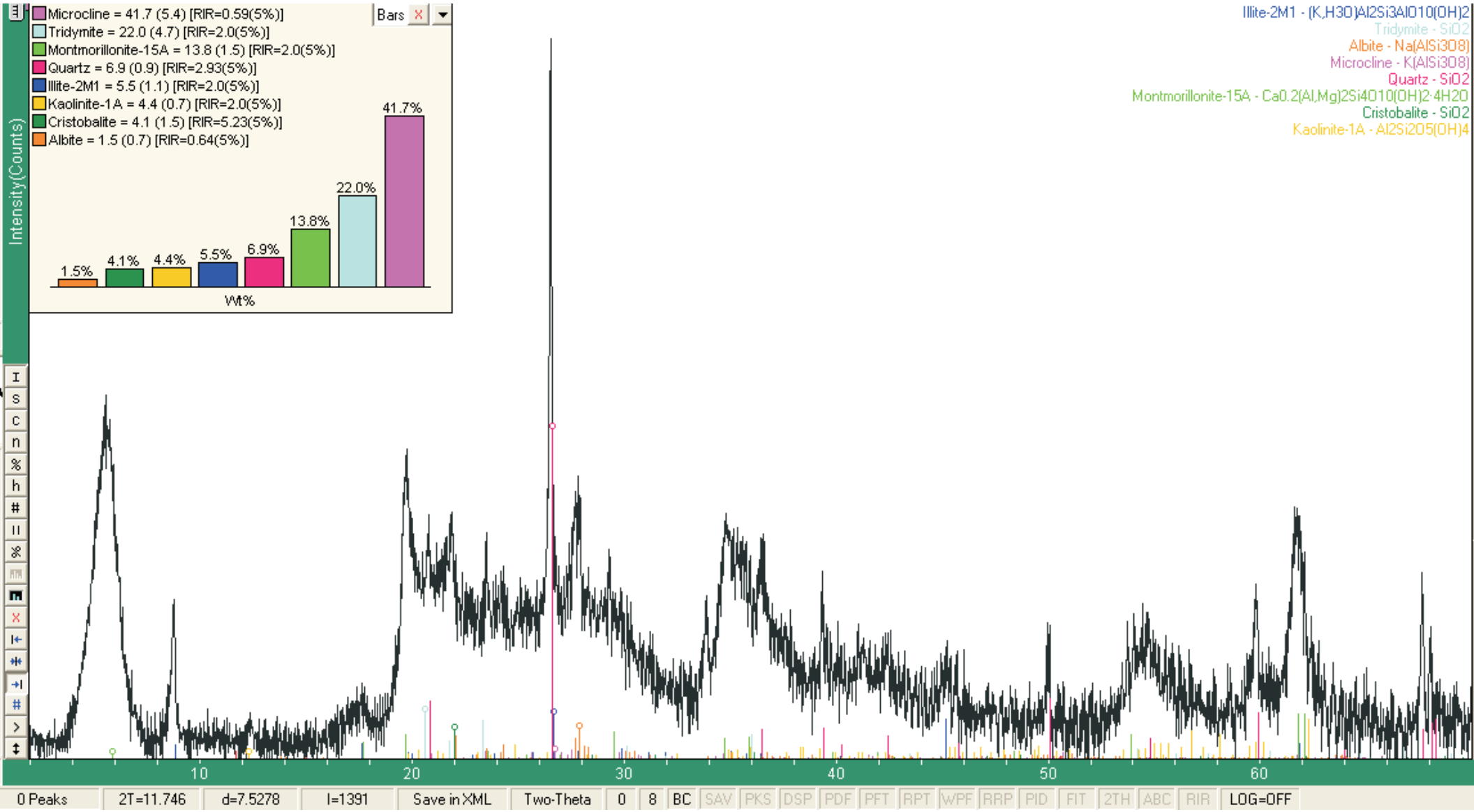

0 Peaks | 2T=11.746 | d=7.5278 | I=1391 | Save in XML | Two-Theta | 0 | 8 | BC | SAV | PKS | DSP | PDF | PFT | RPT | WPF | RRP | PID | FIT | 2TH | ABC | RIR | LOG=OFF

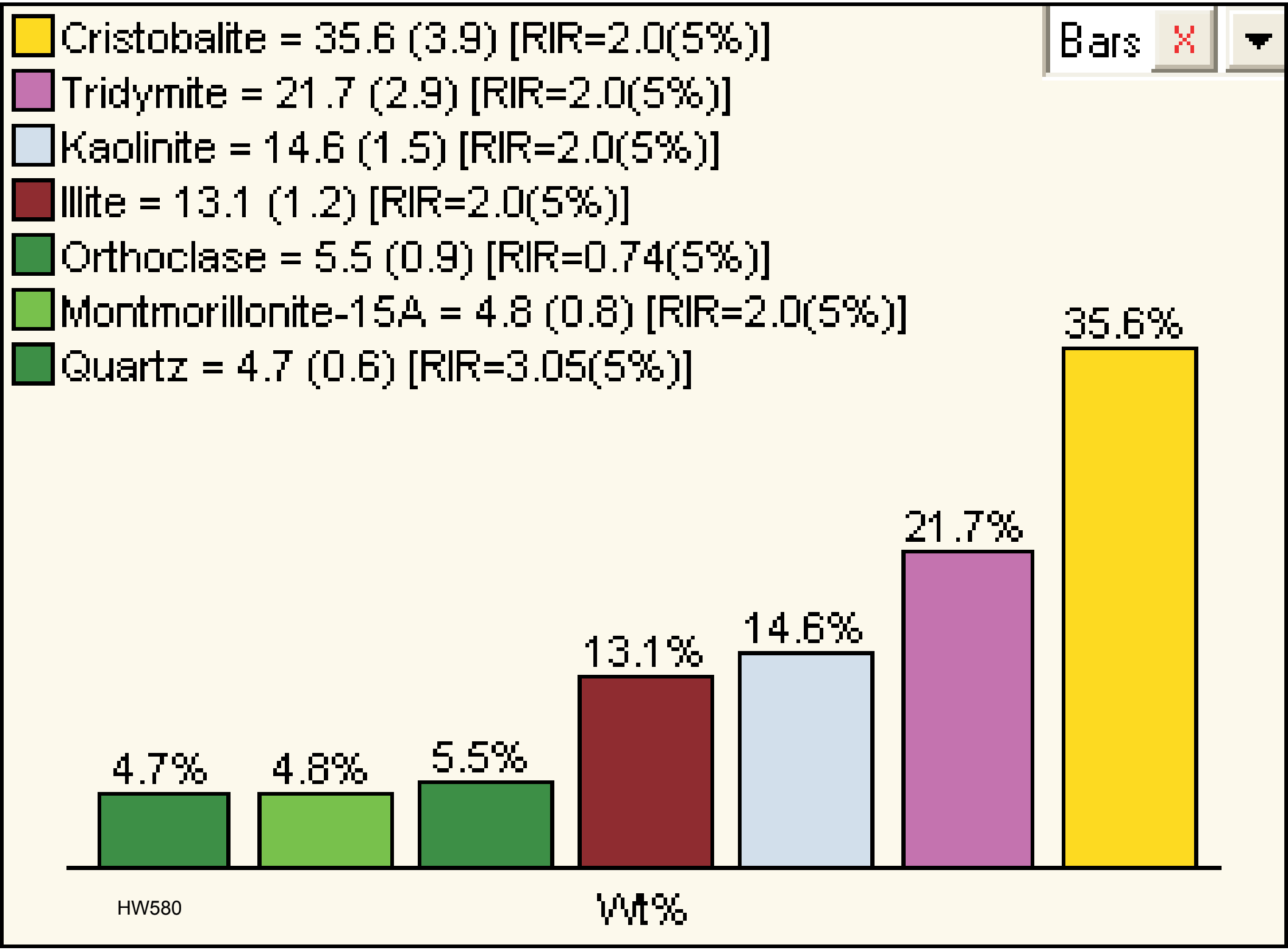
Cristobalite = 35.6 (3.9) [RIR=2.0(5%)]
Tridymite = 21.7 (2.9) [RIR=2.0(5%)]
Kaolinite = 14.6 (1.5) [RIR=2.0(5%)]
Illite = 13.1 (1.2) [RIR=2.0(5%)]
Orthoclase = 5.5 (0.9) [RIR=0.74(5%)]
Montmorillonite-15A = 4.8 (0.8) [RIR=2.0(5%)]
Quartz = 4.7 (0.6) [RIR=3.05(5%)]
Bars
4.7%
4.8%
5.5%
13.1%
14.6%
21.7%
35.6%
HW580
Wt%

HW580

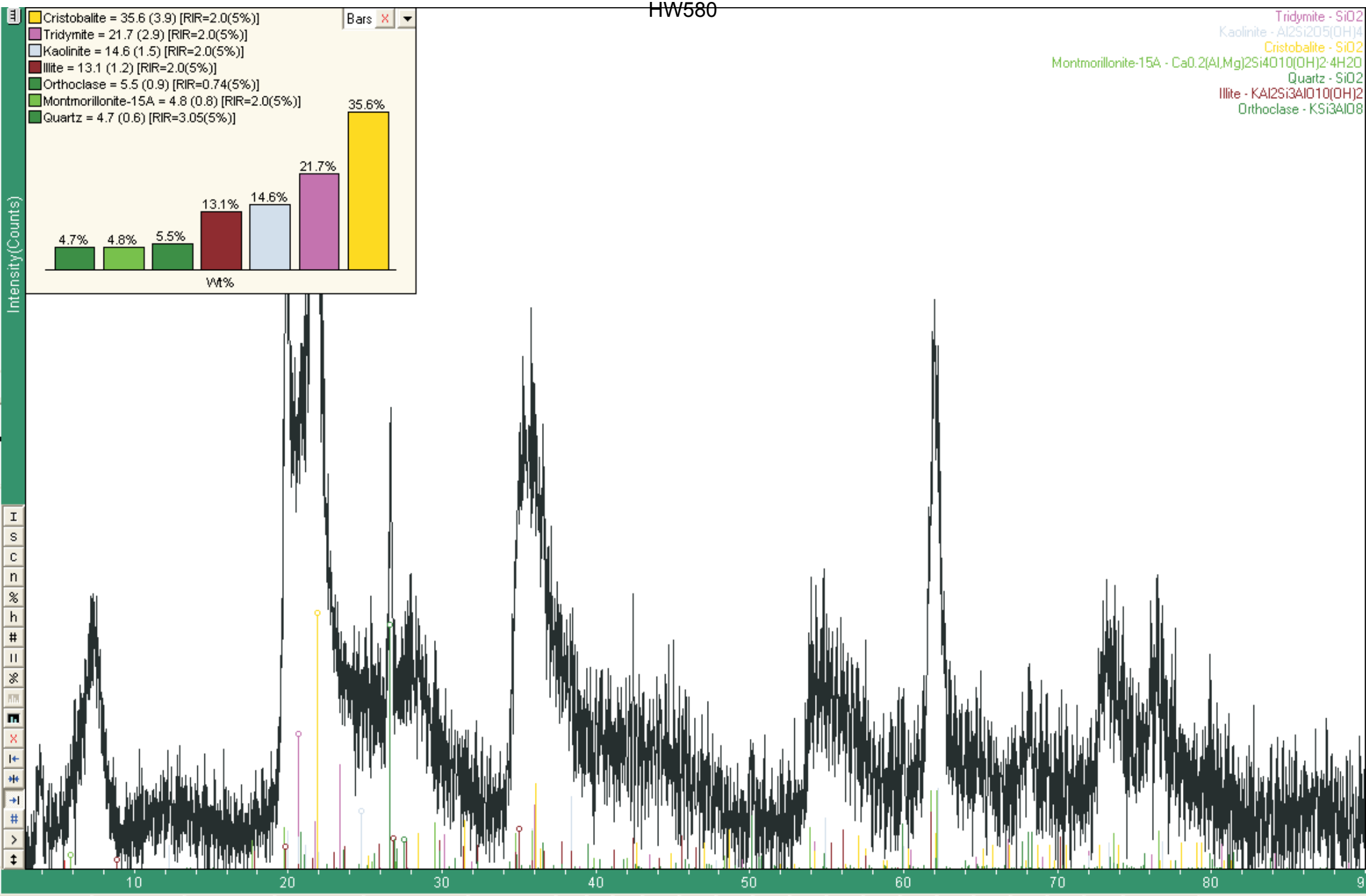

0 Peaks | T=5.525 | d=15.982 | I=309.4 | Save in XML | Theta(deg) | 0 | 7 | BC | SAV | PKS | DSP | PDF | PFT | RPT | WPF | RRP | PID | FIT | 2TH | ABC | RIR | LOG=OFF